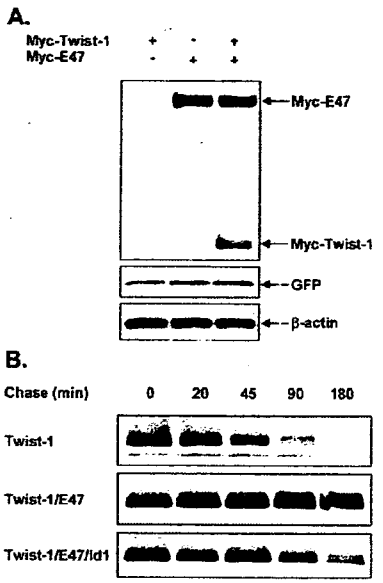

Fig. 5. Twist-1 protein stability is increased by the formation of a heterodimer complex with E47. (A) Myc-tagged Twist-1 and E47 constructs and GFP expression vector were transfected into COS-7 cells. Western blot analysis was performed with anti-Myc antibody. To show transfection efficiency, GFP protein was also detected by western blot. (B) COS-7 cells were transfected with the Flag-tagged Twist-1, Myc-tagged E47 and/or Myc-tagged Id1. At 24 hours after transfection, cells were pulsed with [^{35}S]methionine and cysteine for 3 hours, and chased with unlabeled medium for the indicated times. Labeled cell lysates were immunoprecipitated using anti-Flag antibody. Flag-tagged Twist-1 was visualized using SDS-PAGE.

possibility using immunoprecipitation assay in COS-7 cells. Increasing doses of Id1 decreased the amounts of E47 co-immunoprecipitated with Twist-1 (Fig. 6A). The amount of immunoprecipitated Twist-1 was also decreased by co-transfection of Id1, suggesting that Id1 induces Twist-1 degradation by sequestering E47 from Twist-1.

To examine whether Twist-1 also interferes with Id1-E47 heterodimer formation, we next performed the same experiment by replacing Id1 with Twist-1. In contrast to Id1, Twist-1 failed to interfere with Id1-E47 heterodimer formation (Fig. 6B). These results suggest that Id1 interacts with E47 more strongly than Twist-1 does, resulting in sequestration of E47 from Twist-1. In C3H10T1/2, endogenous Id1 was also co-immunoprecipitated with E47 using anti-E47 antibody (Fig. 6C). We examined the possibility that Id1 could rescue the inhibitory effect of Twist-1 on BMP signaling by inducing Twist-1 degradation. Twist-1-induced inhibition of BMP signaling was overcome by Id1 in a dose-dependent manner (Fig. 6D). It has been reported that differentiation of osteoblastic cells is promoted by transient expression of Id1 in early developmental stages (Peng et al., 2004). We attempted to rescue the inhibition of BMP signaling by Id1 gene transfer to MC3T3-E1-Tw1. As shown in Fig. 6E, the recovery of ALP activity in MC3T3-E1-Tw1 by Id1 gene transfer was significantly higher than by GFP gene transfer. These findings indicate that Id1 may regulate BMP signaling through a positive feedback loop that represses Twist-1 function.

Discussion

During embryonic mesoderm development, BMPs play critical roles in the commitment of mesenchymal cells into osteoblast and chondroblast lineages (Centrella et al., 1994; Hogan, 1996). Smads phosphorylated by BMP stimulation translocate into the nucleus and interact in transcription complexes with several DNA-binding transcription factors or cofactors that affect gene activation (Derynck and Zhang, 2003; Massague, 2000; Wrana, 2000). These factors have been considered critical for a variety of responses to BMP signaling in different BMP-targeted genes. Also, several inhibitors of BMP signaling have been reported. For example, Smad6 inhibits BMP/Smad1 signaling by acting as a selective Smad4 decoy (Hata et al., 1998). Tob, a member of the anti-proliferative protein family, binds Smad1, Smad5 and Smad8, and inhibits Smad-mediated transcriptional activities (Yoshida et al., 2000). Smads have also been shown to interact with bHLH transcription factors. For example, Smad3 directly interacts with MyoD and represses transcriptional activity (Liu et al., 2001). Neurogenin, another bHLH transcription factor, binds to both Smad1 and CBP (CREB-binding protein), and inhibits glial differentiation (Sun et al., 2001). The present study provides the first report that Twist-1, a DNA-binding bHLH transcription factor, inhibits transcriptional activities mediated by Smads (Fig. 3A,B,D).

Twist-1 reportedly acts as an inhibitor of muscle differentiation by sequestering E-protein from MyoD and blocking DNA binding, and by inhibiting trans-activation by MEF2 (Spicer et al., 1996). Twist-2 also requires heterodimerization with E-protein for inhibition of MyoD and MEF2 (Gong and Li, 2002), as seen with Twist-1. In addition, HDACs are involved in the repression of MyoD by Twist-1 and -2. In our results, Twist-1 also required heterodimerization with E47 for both maximal inhibition of Smad-mediated transcriptional activity (Fig. 3A,B,D) and increasing Twist-1 protein stability (Fig. 5B). BMPs activate transcription through physical interaction and functional cooperation of R-Smads and coactivators CBP and/or p300 (Derynck and Zhang, 2003). Our result (Fig. 4A,B) supports the possibility that the inhibition of BMP signaling by Twist-1 and E47 was mediated by direct recruitment of HDAC1 to Smad complexes via Smad4. The repression of HDAC by TSA increased the expression of osteogenic factors probably by the activation of BMP signaling. However, gel-shift assay of Smads revealed that Twist-1 failed in the inhibition of DNA binding of Smads (data not shown). This result was not contradictory to the involvement of HDAC in inhibitory mechanism by Twist-1.

We also showed that the effect of Twist-1 in repressing BMP signaling was abrogated by Id1 (Fig. 6D,E). Id1 expression is induced by BMP stimulation in mesenchymal and neuroepithelial cells (Katagiri et al., 1994; Nakashima et al., 2001; Ogata et al., 1993). Id1 lacks the basic region necessary for binding to the E-box and acts as a dominant negative regulator by sequestering E-protein (Benezra et al., 1990). Furthermore, Id1 sequesters E-proteins away from myogenin and inhibits myogenesis by accelerating myogenin degradation (Vinals and Ventura, 2004). In neural development, transient induction of Id1 by BMP2 decreases Mash1 stability and restricts neuronal differentiation by the same mechanism (Vinals et al., 2004). These findings support the possibility that Id1 may positively regulate BMP signaling

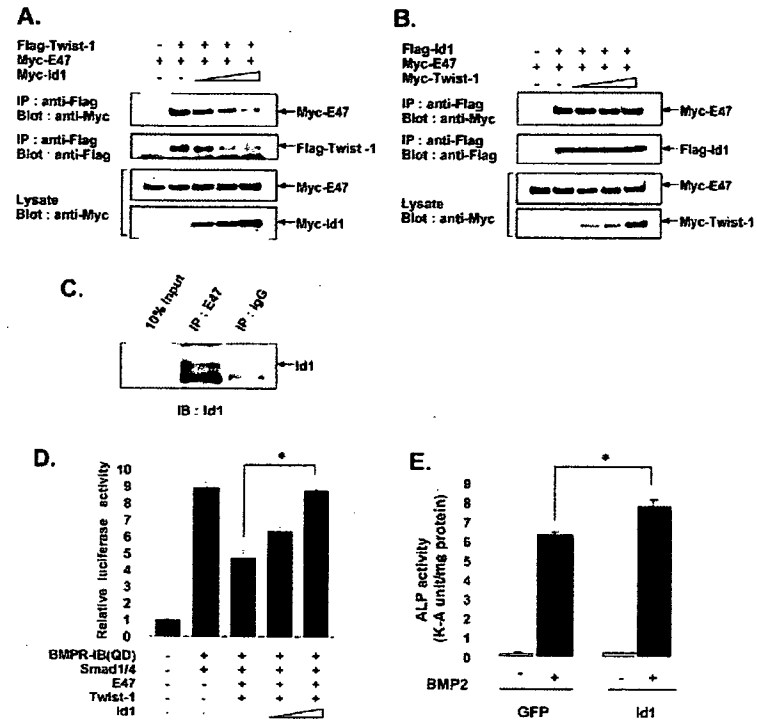

Fig. 6. Id1 inhibits Twist-1 function by sequestering E47 from Twist-1. (A) COS-7 cells were transiently transfected with Flag-Twist-1, Myc-tagged E47 and increasing doses (0.5, 1 or 2 μg) of Myc-tagged Id1 construct. Lysates were immunoprecipitated using anti-Flag antibody and blotted with anti-Flag and anti-Myc-antibody. (B) COS-7 cells were transiently transfected with Flag-Id1, Myc-tagged E47 and increasing doses (0.5, 1 or 2 μg) of Myc-tagged Twist-1 construct. Lysates were immunoprecipitated using anti-Flag antibody and blotted with anti-Flag and anti-Myc-antibody. (C) Endogenous E47 in C3H10T1/2 cells was precipitated using anti-E47 antibody. Then, Id1 was detected in the immunoprecipitates by western blot. (D) P19 cells were transiently transfected with 3GC2-Lux luciferase construct in combination with 50 ng of BMPR-IB(QD), Smad1 and Smad4, 25 ng of Twist-1 and E47, and increasing doses (25 or 100 ng) of Id1 expression construct. Cells were lysed and luciferase activity was assayed 24 hours after transfection (*P<0.01). (E) MC3T3-E1-Tw1 cells were transiently transfected with either Id1 or GFP expression construct by electroporation (Amaxa). The cells were grown in the presence or absence of rhBMP2 (300 ng/ml) for 6 days. ALP activity was measured as described in the Materials and Methods. Data are presented as mean ± s.d. of triplicate samples (*P<0.05).

by sequestering E-protein from Twist-1 to accelerate degradation. As shown in Fig. 6E, the recovery of ALP activity in MC3T3-E1-Tw1 by Id1 gene transfer was significantly higher than by GFP gene transfer, but the effect was not as much as expected from co-transfection experiment (Fig. 6D). We estimated that transient expression of Id1 was not sufficient to completely overcome the effect of stably expressing Twist-1, because transfection efficiency was not as high (at most 20%) in MC3T3-E1 cells.

In response to BMP stimulation, C3H10T1/2 embryonic mesenchymal cells express bone markers including collagen type I, ALP, osteopontin and osteocalcin (Ju et al., 2000). The osteopontin gene is reportedly a target of the BMP signaling pathway. Smad1 activates the osteopontin promoter by preventing Hoxc-8 (which negatively regulates osteopontin expression) from binding to this promoter (Shi et al., 1999; Yang et al., 2000). In addition, BMP stimulates direct binding of Smad proteins to the targeting sequence of the osteopontin promoter and activates transcription (Hullinger et al., 2001). In this study, we found that overexpression of Twist-1 repressed BMP2-induced expression of osteopontin and osteocalcin, and ALP activity (Fig. 1B,C). It is also known that Runx2 activates the expression of ALP, osteopontin and osteocalcin (Ducy et al., 1997; Harada et al., 1999). Furthermore, Twist-1 directly inhibits Runx2 (Bialek et al., 2004). From these reports, there is a possibility that the inhibition of BMP signaling in our experiments might result from an indirect effect mediated by the inhibition of Runx2. However, by direct binding with Runx2, Smads activate the transcription of Runx2 (Lee et al., 2000; Zhang et al., 2000). Moreover, BMP signaling was suppressed in co-transfection experiments using a reporter gene without the Runx2 recognition DNA sequence, as shown in Fig. 3A,B. Therefore, in addition to an indirect effect, through the inhibition of Runx2, it is likely that Twist-1 may have a direct inhibitory effect on BMP signaling.

We also showed that Smad-dependent transcriptional activity was enhanced by siRNA-mediated downregulation of endogenous Twist-1 in transient transfection analysis with a reporter construct containing BMP-responsive elements (Fig. 2B,C). Levels of Twist-1 expression gradually decrease during osteoblast differentiation (Bialek et al., 2004; Rice et al., 2000; Tamura and Noda, 1999). Taken together these results indicate that Twist-1 may maintain the population of undifferentiated mesenchymal cells by inhibiting BMP-induced osteoblast differentiation. Our data indicate a novel mechanism by which the cellular effects of BMP signals can be potentially regulated through direct competition between Twist-1 and Id1 for binding to E-protein.

Materials and Methods

Plasmid construction

Mouse Twist-1, E47, Id1 and Smad1 and Smad4 were amplified using polymerase chain reaction (PCR) from cDNA templates, which were reverse transcribed from mRNA of C3H10T1/2. To create mammalian expression vectors Myc-Twist-1, E47, Id1, Flag-Twist-1, Smad1 and Smad4, cDNA clones were introduced using Gateway technology (Invitrogen, San Diego, CA) into pCAGIP-Myc and pCAGIP-Flag vectors (Niwa et al., 2002). For Flag-Twist-1 deletion mutants, Twist-NBCT (deletion of amino acids 125-169) were created by PCR, then introduced into pCAGIP-Flag using Gateway technology. To generate mammalian expression vectors pCMV-Twist-1, pCMV-E47, pCMV-Id1 and pCMV-Smad1 and pCMV-Smad4, the corresponding cDNA clones were introduced with Gateway technology into pcDNA3.1 (Invitrogen), which was converted into the destination vector. A 3GC2-Lux luciferase construct, the constitutively active form of BMP type I receptor [BMPR-IB(QD)] (Imamura et al., 1997) and the constitutively active form of TGF-β type I receptor [TβR-I(TD)] (Wieser et al., 1995) were kindly donated by Kohei Miyazono (University of Tokyo).

Cell culture and stable transfection

The C3H10T1/2 murine mesenchymal progenitor cell line, MC3T3E-1 osteoblastic cell line and COS-7 African green monkey SV40-transformed kidney fibroblast

cells line were cultured in Dulbecco's modified Eagle's medium (DMEM) supplemented with 10% heat-inactivated fetal bovine serum (FBS) and antibiotics. The P19 murine teratocarcinoma cell line was cultured in α-modified Eagle's medium supplemented with 10% FBS and antibiotics. Twist-1-overexpressing MC3T3-E1 (MC3T3-E1-Tw1) cells were obtained by puromycin selection of MC3T3-E1 cells transfected with pCAGIP-Flag-Twist-1. Screening of Twist-1-overexpressing clones was performed by western blotting of immunoprecipitates using anti-Flag antibody.

siRNA method

Target short interfering RNA (siRNA) was determined using the siRNA design tool (Invitrogen). The siTwist-604 sense sequence was 5′-AAGCUGAGCAAGAUUCAGACC-3′; siTwist-691 sense sequence was 5′-AAGAUGGCAAGCUGCAGCUAU-3′; siTwist-645 sense sequence was 5′-CAUCGACUUCCUGUACCAGGU-3′; and siTwist-481 sense sequence was 5′-CAGUCGUACGAGGAGCUGCAG-3′. As a control, the non-silencing siRNA sense sequence was 5′-AAGCGCGCUUUGUAGGAUUCG-3′. C3H10T1/2 cells were seeded at 70% confluence on the day before transfection. Transfections were performed using Lipofectamine 2000 transfection reagent (Invitrogen). To examine the effects of Twist-1-specific siRNA on reporter constructs, cells were transfected with 3GC2-Lux and pRL-TK vector (Promega, Madison, WI) using FuGENE6 transfection reagent (Roche, Basel, Switzerland) 24 hours after siRNA transfection. At 36 hours after siRNA transfection, cells were treated with rhBMP2 (300 ng/ml) for 12 hours. Both firefly and *Renilla* luciferase activities were measured 2 days after siRNA transfection using a dual luciferase assay system (Promega). Co-transfections of siRNA and plasmid DNAs were performed using X-treamGENE siRNA transfection reagent (Roche).

RNA extraction and northern blot analysis

Total RNA was isolated using Isogen (Nippon Gene, Tokyo, Japan) according to the instructions of the manufacturer. Total RNA (15 μg) was denatured, electrophoresed in 2% agarose gels containing 18% formaldehyde, then transferred to Hybond-N+ membrane (Amersham Biosciences, Piscataway, NJ). Membranes were hybridized at 65°C for 12 hours in a hybridization buffer, PerfectHyb (Toyobo, Osaka Japan). Probes for Twist-1, osteocalcin, osteopontin and G3PDH were labeled using the RadPrime DNA labeling system (Invitrogen). After hybridization, membranes were washed four times with 2× standard sodium citrate (SSC) and 0.1% sodium dodecyl sulfate (SDS). Blots were exposed to X-ray films using intensify screens at –80°C.

Alkaline phosphatase assay

Alkaline phosphatase (ALP) activity was assessed as previously described (Wakabayashi et al., 2002). Briefly, cell lysates were centrifuged and supernatants were used for enzyme assays. ALP activity was measured according to the methods of Kind-King, using a test kit (Wako, Osaka, Japan) with phenylphosphate as a substrate. Enzyme activity was expressed in King-Armstrong (K-A) units, normalized to protein concentration. Results are presented as mean ± standard deviation (s.d.) from a representative experiment. Statistical analysis was performed using analysis of variance (ANOVA).

Transfections and reporter assays

P19 cells were transiently transfected using 3GC2-Lux together with expression constructs of Smad1, Smad4, Twist-1, E47, Id1 and BMPR-IB(QD) using FuGENE6 transfection reagent. P19 cells were chosen because the cells responded to BMPs and expressed some of the BMP target genes. Additionally, transfection efficiency was higher in P19 cells than in other cell lines. At 24 hours after transfection, both firefly and *Renilla* luciferase activities were assayed with the dual luciferase assay system (Promega) using a Lumat LB 9507 luminometer (Berthold Technologies, Wildbad, Germany). Firefly luciferase activity was normalized with respect to *Renilla* luciferase activity. All assays were performed at least three times in duplicate or triplicate. Results are presented as mean ± s.d. from a representative experiment. Statistical analysis was performed using ANOVA.

Immunoprecipitation and immunoblotting

COS-7 cells were transiently transfected with the expression construct using FuGENE6 transfection reagent. COS-7 cells were used because they contained no endogenous Twist-1. At 24 hours after transfection, cells were lysed in buffer containing 25 mM Hepes pH 8.0, 150 mM KCl, 2 mM EDTA, 0.1% Nonidet P-40 (NP-40) and EDTA-free complete protease inhibitor cocktail (Roche). After 20 minutes on ice, cell lysates were pelleted by centrifugation and supernatants were pre-cleared with normal mouse IgG (Santa Cruz, Santa Cruz, CA) for 30 minutes at 4°C, then incubated with anti-FLAG M2 affinity gel (Sigma, St Louis, MO) for 4 hours at 4°C. Immunoprecipitates were washed four times with the buffer used for cell solubilization. Immune complexes were eluted at 98°C for 5 minutes in Laemmli's sample buffer. Immunoprecipitates were separated by SDS-polyacrylamide gel electrophoresis (PAGE), transferred to polyvilinidendifluoride (PVDF) membrane, and immunoblotted with anti-Flag M2 antibody (Sigma) and anti-Myc antibody (MBL, Nagoya Japan). Protein bands were visualized using Chemi-Lumi One (Nacalai Tesque, Kyoto, Japan).

To detect overexpressed Smad1 and Smad4, P19 cells were lysed as described above, 24 hours after transfection. Lysates were separated by SDS-PAGE, transferred to PVDF membrane, and immunoblotted with anti-Smad1 and -Smad4 antibody (Santa Cruz) and anti-β-actin antibody (ABcam, Cambrige, UK). Protein bands were visualized using Chemi-Lumi One (Nacalai Tesque).

Nuclear protein extracts were prepared from MC3T3-E1 cells as follows. Cells were harvested by centrifugation at 500 *g* for 10 minutes at 4°C. Cell pellets were washed by gentle resuspension in cold PBS-0.5 mM EDTA and nuclei isolation buffer (NIB) containing 10 mM Tris-HCl (pH 7.5), 60 mM KCl, 15 mM NaCl, 1.5 mM $MgCl_2$, 1 mM $CaCl_2$, 0.25 M sucrose, 10% glycerol, 0.1 mM phenylmethylsulfonylfluoride (PMSF) and EDTA-free complete protease inhibitor cocktail (Roche). Cells were re-suspended with ice-cold NIB containing 0.1% NP-40 and allowed to swell for 10 minutes on ice. Swollen cells were centrifuged at 500 *g* for 10 minutes at 4°C. Nuclei pellets were washed in cold NIB and centrifuged at 500 *g* for 5 minutes at 4°C. Nuclear pellets were diluted to 1.5 mg/ml DNA with ice-cold NIB and digested using micrococcal nuclease (80 units/mg DNA; Worthington, Lakewood, NJ). Digested nuclei were rapidly cooled on ice for 10 minutes and centrifuge at 12,800 *g* for 10 minutes at 4°C. Supernatant (S1) was collected and pellets were re-suspended with ice-cold cell lysis buffer containing 10 mM Tris-HCl (pH 7.5), 2 mM EDTA, 10% glycerol, 300 mM NaCl, 0.1 mM PMSF and EDTA-free complete protease inhibitor cocktail (Roche), then incubated for 45 minutes on ice. Nuclear debris was spun out by centrifugation at 12,800 *g* for 10 minutes at 4°C, and the supernatant (S2) was collected. S1 and S2 fractions were combined, then incubated with anti-Flag M2 affinity gel (Sigma) for 4 hours at 4°C. Immunoprecipitates were washed four times with cell lysis buffer containing 0.1% NP-40. Immune complexes were eluted at 98°C for 5 minutes in Laemmli's sample buffer. Immunoprecipitates were separated by SDS-PAGE, transferred to PVDF membrane, and immunoblotted using anti-Flag M2 antibody (Sigma).

To analyze the interaction of Id1 and E47, or Smad4, HDAC1 and Flag-Twist-1, C3H10T1/2 and MC3T3-E1-Tw1 cells were lysed with RIPA buffer containing 50 mM Tris-HCl (pH 7.4), 1% NP-40, 0.25% sodium deoxycholate, 150 mM NaCl, 1 mM EDTA and EDTA-free complete protease inhibitor cocktail (Roche), and the supernatant was obtained by centrifugation of the lysates at 12,800 *g* for 5 minutes at 4°C. After the removal of non-specifically bound substances using non-immune IgG (Santa Cruz), the supernatant was incubated with anti-E47 (Santa Cruz) antibody for 2 hours at 4°C and precipitated with protein A beads, or anti-Flag M2 affinity gel for 4 hours at 4°C. After washing the precipitates four times with the RIPA buffer, immune complexes were eluted at 98°C for 5 minutes in Laemmli's sample buffer. Immunoprecipitates were separated by SDS-PAGE, transferred to PVDF membrane, and immunoblotted using anti-Id1, anti-Smad4 (Santa Cruz), anti-Smad1 (Zymed, San Francisco, CA), anti-HDAC1(Upstate Temecula, CA) antibodies.

Pulse-chase assay

Pulse-chase assay was performed according to the method previously described (Deed et al., 1996), with minor modification. COS-7 cells were transfected with Flag-Twist-1, Myc-E47 and Myc-Id1 using FuGENE6 transfection reagent. At 24 hours after transfection, cells were starved in cysteine and methionine-free DMEM (Invitrogen) containing with 5% dialyzed FBS for 1 hour, then incubated for an additional 2 hours in cysteine and methionine-free DMEM containing 10% dialyzed FBS and 50 μCi/ml of Promix (Amersham). Labeled cells were then incubated in standard DMEM supplemented with 10% FBS and harvested at various time points. Immunoprecipitation was performed as described above.

Real-time quantitative PCR

MC3T3-E1-Tw1 cells (2×10^5 cells) were treated with BMP (600 ng) alone or the mixture of BMP (600 ng) and trichostatin (TSA, 330 nM; Sigma). At 24 hours after the treatment, total RNA was extracted from cells using RNeasy kits (Qiagen, Hilden, Germany) and digested with DNase I according to the manufacturer's instructions. Total RNA (5 μg) was reverse transcribed into cDNA using High Capacity cDNA Archive Kits (Applied Biosystems, Foster City, CA) and amplified by real-time quantitative PCR using an ABI PRISM 7700 Sequence Detection System (Applied Biosystems, Foster City, CA). Mixtures of probes and primer pairs specific for murine ALP, Runx2, osteopontin and GAPDH were purchased from Applied Biosystems (Foster City, CA). The concentration of target genes was determined using the comparative CT method (threshold cycle number at the cross-point between amplification plot and threshold) and values were normalized to an internal GAPDH control. Results are presented as mean ± s.d. from a representative experiment.

We wish to thank K. Miyazono for providing the 3GC2-Lux luciferase construct, BMPR-IB(QD) and TβR-I(TD), and Astellas Pharmaceutical Co. for providing rhBMP2. This work was supported by the Northern Osaka (Saito) Biomedical Knowledge-Based Cluster Creation Project, a Grant-in-Aid from the Ministry of Education,

Culture, Sports, Science and Technology, the Japanese Government, and Takeda Science Foundation.

References

Benezra, R., Davis, R. L., Lockshon, D., Turner, D. L. and Weintraub, H. (1990). The protein Id: a negative regulator of helix-loop-helix DNA binding proteins. *Cell* **61**, 49-59.

Bialek, P., Kern, B., Yang, X., Schrock, M., Sosic, D., Hong, N., Wu, H., Yu, K., Ornitz, D. M., Olson, E. N. et al. (2004). A twist code determines the onset of osteoblast differentiation. *Dev. Cell* **6**, 423-435.

Bourgeois, P., Bolcato-Bellemin, A. L., Danse, J. M., Bloch-Zupan, A., Yoshiba, K., Stoetzel, C. and Perrin-Schmitt, F. (1998). The variable expressivity and incomplete penetrance of the twist-null heterozygous mouse phenotype resemble those of human Saethre-Chotzen syndrome. *Hum. Mol. Genet.* **7**, 945-957.

Centrella, M., Horowitz, M. C., Wozney, J. M. and McCarthy, T. L. (1994). Transforming growth factor-beta gene family members and bone. *Endocr. Rev.* **15**, 27-39.

Chen, Z. F. and Behringer, R. R. (1995). twist is required in head mesenchyme for cranial neural tube morphogenesis. *Genes Dev.* **9**, 686-699.

Deed, R. W., Armitage, S. and Norton, J. D. (1996). Nuclear localization and regulation of Id protein through an E protein-mediated chaperone mechanism. *J. Biol. Chem.* **271**, 23603-23606.

Derynck, R. and Zhang, Y. E. (2003). Smad-dependent and Smad-independent pathways in TGF-beta family signalling. *Nature* **425**, 577-584.

Ducy, P., Zhang, R., Geoffroy, V., Ridall, A. L. and Karsenty, G. (1997). Osf2/Cbfa1: a transcriptional activator of osteoblast differentiation. *Cell* **89**, 747-754.

El Ghouzzi, V., Legeai-Mallet, L., Aresta, S., Benoist, C., Munnich, A., de Gunzburg, J. and Bonaventure, J. (2000). Saethre-Chotzen mutations cause TWIST protein degradation or impaired nuclear location. *Hum. Mol. Genet.* **9**, 813-819.

Gong, X. Q. and Li, L. (2002). Dermo-1, a multifunctional basic helix-loop-helix protein, represses MyoD transactivation via the HLH domain, MEF2 interaction, and chromatin deacetylation. *J. Biol. Chem.* **277**, 12310-12317.

Hamamori, Y., Wu, H. Y., Sartorelli, V. and Kedes, L. (1997). The basic domain of myogenic basic helix-loop-helix (bHLH) proteins is the novel target for direct inhibition by another bHLH protein, Twist. *Mol. Cell. Biol.* **17**, 6563-6573.

Hamamori, Y., Sartorelli, V., Ogryzko, V., Puri, P. L., Wu, H. Y., Wang, J. Y., Nakatani, Y. and Kedes, L. (1999). Regulation of histone acetyltransferases p300 and PCAF by the bHLH protein twist and adenoviral oncoprotein E1A. *Cell* **96**, 405-413.

Harada, H., Tagashira, S., Fujiwara, M., Ogawa, S., Katsumata, T., Yamaguchi, A., Komori, T. and Nakatsuka, M. (1999). Cbfa1 isoforms exert functional differences in osteoblast differentiation. *J. Biol. Chem.* **274**, 6972-6978.

Hata, A., Lagna, G., Massague, J. and Hemmati-Brivanlou, A. (1998). Smad6 inhibits BMP/Smad1 signaling by specifically competing with the Smad4 tumor suppressor. *Genes Dev.* **12**, 186-197.

Hebrok, M., Fuchtbauer, A. and Fuchtbauer, E. M. (1997). Repression of muscle-specific gene activation by the murine Twist protein. *Exp. Cell Res.* **232**, 295-303.

Hogan, B. L. (1996). Bone morphogenetic proteins: multifunctional regulators of vertebrate development. *Genes Dev.* **10**, 1580-1594.

Hullinger, T. G., Pan, Q., Viswanathan, H. L. and Somerman, M. J. (2001). TGFbeta and BMP-2 activation of the OPN promoter: roles of smad- and hox-binding elements. *Exp. Cell Res.* **262**, 69-74.

Imamura, T., Takase, M., Nishihara, A., Oeda, E., Hanai, J., Kawabata, M. and Miyazono, K. (1997). Smad6 inhibits signalling by the TGF-beta superfamily. *Nature* **389**, 622-626.

Ishida, W., Hamamoto, T., Kusanagi, K., Yagi, K., Kawabata, M., Takehara, K., Sampath, T. K., Kato, M. and Miyazono, K. (2000). Smad6 is a Smad1/5-induced smad inhibitor. Characterization of bone morphogenetic protein-responsive element in the mouse Smad6 promoter. *J. Biol. Chem.* **275**, 6075-6079.

Ju, W., Hoffmann, A., Verschueren, K., Tylzanowski, P., Kaps, C., Gross, G. and Huylebroeck, D. (2000). The bone morphogenetic protein 2 signaling mediator Smad1 participates predominantly in osteogenic and not in chondrogenic differentiation in mesenchymal progenitors C3H10T1/2. *J. Bone Miner. Res.* **15**, 1889-1899.

Katagiri, T., Yamaguchi, A., Komaki, M., Abe, E., Takahashi, N., Ikeda, T., Rosen, V., Wozney, J. M., Fujisawa-Sehara, A. and Suda, T. (1994). Bone morphogenetic protein-2 converts the differentiation pathway of C2C12 myoblasts into the osteoblast lineage. *J. Cell Biol.* **127**, 1755-1766.

Lassar, A. B., Davis, R. L., Wright, W. E., Kadesch, T., Murre, C., Voronova, A., Baltimore, D. and Weintraub, H. (1991). Functional activity of myogenic HLH proteins requires hetero-oligomerization with E12/E47-like proteins in vivo. *Cell* **66**, 305-315.

Lee, K. S., Kim, H. J., Li, Q. L., Chi, X. Z., Ueta, C., Komori, T., Wozney, J. M., Kim, E. G., Choi, J. Y., Ryoo, H. M. et al. (2000). Runx2 is a common target of transforming growth factor beta1 and bone morphogenetic protein 2, and cooperation between Runx2 and Smad5 induces osteoblast-specific gene expression in the pluripotent mesenchymal precursor cell line C2C12. *Mol. Cell. Biol.* **20**, 8783-8792.

Lee, M. S., Lowe, G. N., Strong, D. D., Wergedal, J. E. and Glackin, C. A. (1999). TWIST, a basic helix-loop-helix transcription factor, can regulate the human osteogenic lineage. *J. Cell. Biochem.* **75**, 566-577.

Leptin, M. (1991). twist and snail as positive and negative regulators during Drosophila mesoderm development. *Genes Dev.* **5**, 1568-1576.

Li, L., Cserjesi, P. and Olson, E. N. (1995). Dermo-1: a novel twist-related bHLH protein expressed in the developing dermis. *Dev. Biol.* **172**, 280-292.

Liu, D., Black, B. L. and Derynck, R. (2001). TGF-beta inhibits muscle differentiation through functional repression of myogenic transcription factors by Smad3. *Genes Dev.* **15**, 2950-2966.

Massague, J. (2000). How cells read TGF-beta signals. *Nat. Rev. Mol. Cell Biol.* **1**, 169-178.

Murre, C., McCaw, P. S. and Baltimore, D. (1989). A new DNA binding and dimerization motif in immunoglobulin enhancer binding, daughterless, MyoD, and myc proteins. *Cell* **56**, 777-783.

Nakashima, K., Takizawa, T., Ochiai, W., Yanagisawa, M., Hisatsune, T., Nakafuku, M., Miyazono, K., Kishimoto, T., Kageyama, R. and Taga, T. (2001). BMP2-mediated alteration in the developmental pathway of fetal mouse brain cells from neurogenesis to astrocytogenesis. *Proc. Natl. Acad. Sci. USA* **98**, 5868-5873.

Niwa, H., Masui, S., Chambers, I., Smith, A. G. and Miyazaki, J. (2002). Phenotypic complementation establishes requirements for specific POU domain and generic transactivation function of Oct-3/4 in embryonic stem cells. *Mol. Cell. Biol.* **22**, 1526-1536.

Ogata, T., Wozney, J. M., Benezra, R. and Noda, M. (1993). Bone morphogenetic protein 2 transiently enhances expression of a gene, Id (inhibitor of differentiation), encoding a helix-loop-helix molecule in osteoblast-like cells. *Proc. Natl. Acad. Sci. USA* **90**, 9219-9222.

Peng, Y., Kang, Q., Luo, Q., Jiang, W., Si, W., Liu, B. A., Luu, H. H., Park, J. K., Li, X., Luo, J. et al. (2004). Inhibitor of DNA binding/differentiation helix-loop-helix proteins mediate bone morphogenetic protein-induced osteoblast differentiation of mesenchymal stem cells. *J. Biol. Chem.* **279**, 32941-32949.

Rice, D. P., Aberg, T., Chan, Y., Tang, Z., Kettunen, P. J., Pakarinen, L., Maxson, R. E. and Thesleff, I. (2000). Integration of FGF and TWIST in calvarial bone and suture development. *Development* **127**, 1845-1855.

Shi, X., Yang, X., Chen, D., Chang, Z. and Cao, X. (1999). Smad1 interacts with homeobox DNA-binding proteins in bone morphogenetic protein signaling. *J. Biol. Chem.* **274**, 13711-13717.

Spicer, D. B., Rhee, J., Cheung, W. L. and Lassar, A. B. (1996). Inhibition of myogenic bHLH and MEF2 transcription factors by the bHLH protein Twist. *Science* **272**, 1476-1480.

Sun, X. H. and Baltimore, D. (1991). An inhibitory domain of E12 transcription factor prevents DNA binding in E12 homodimers but not in E12 heterodimers. *Cell* **64**, 459-470.

Sun, X. H., Copeland, N. G., Jenkins, N. A. and Baltimore, D. (1991). Id proteins Id1 and Id2 selectively inhibit DNA binding by one class of helix-loop-helix proteins. *Mol. Cell. Biol.* **11**, 5603-5611.

Sun, Y., Nadal-Vicens, M., Misono, S., Lin, M. Z., Zubiaga, A., Hua, X., Fan, G. and Greenberg, M. E. (2001). Neurogenin promotes neurogenesis and inhibits glial differentiation by independent mechanisms. *Cell* **104**, 365-376.

Tamura, M. and Noda, M. (1999). Identification of DERMO-1 as a member of helix-loop-helix type transcription factors expressed in osteoblastic cells. *J. Cell. Biochem.* **72**, 167-176.

Thies, R. S., Bauduy, M., Ashton, B. A., Kurtzberg, L., Wozney, J. M. and Rosen, V. (1992). Recombinant human bone morphogenetic protein-2 induces osteoblastic differentiation in W-20-17 stromal cells. *Endocrinology* **130**, 1318-1324.

Thisse, B., el Messal, M. and Perrin-Schmitt, F. (1987). The twist gene: isolation of a Drosophila zygotic gene necessary for the establishment of dorsoventral pattern. *Nucleic Acids Res.* **15**, 3439-3453.

Urist, M. R. (1965). Bone: formation by autoinduction. *Science* **150**, 893-899.

Vinals, F. and Ventura, F. (2004). Myogenin protein stability is decreased by BMP-2 through a mechanism implicating Id1. *J. Biol. Chem.* **279**, 45766-45772.

Vinals, F., Reiriz, J., Ambrosio, S., Bartrons, R., Rosa, J. L. and Ventura, F. (2004). BMP-2 decreases Mash1 stability by increasing Id1 expression. *EMBO J.* **23**, 3527-3537.

Wakabayashi, S., Tsutsumimoto, T., Kawasaki, S., Kinoshita, T., Horiuchi, H. and Takaoka, K. (2002). Involvement of phosphodiesterase isozymes in osteoblastic differentiation. *J. Bone Miner. Res.* **17**, 249-256.

Wieser, R., Wrana, J. L. and Massague, J. (1995). GS domain mutations that constitutively activate T beta R-I, the downstream signaling component in the TGF-beta receptor complex. *EMBO J.* **14**, 2199-2208.

Wolf, C., Thisse, C., Stoetzel, C., Thisse, B., Gerlinger, P. and Perrin-Schmitt, F. (1991). The M-twist gene of Mus is expressed in subsets of mesodermal cells and is closely related to the Xenopus X-twi and the Drosophila twist genes. *Dev. Biol.* **143**, 363-373.

Wrana, J. L. (2000). Regulation of Smad activity. *Cell* **100**, 189-192.

Wrana, J. L., Attisano, L., Carcamo, J., Zentella, A., Doody, J., Laiho, M., Wang, X. F. and Massague, J. (1992). TGF beta signals through a heteromeric protein kinase receptor complex. *Cell* **71**, 1003-1014.

Yang, X., Ji, X., Shi, X. and Cao, X. (2000). Smad1 domains interacting with Hoxc-8 induce osteoblast differentiation. *J. Biol. Chem.* **275**, 1065-1072.

Yoshida, Y., Tanaka, S., Umemori, H., Minowa, O., Usui, M., Ikematsu, N., Hosoda, E., Imamura, T., Kuno, J., Yamashita, T. et al. (2000). Negative regulation of BMP/Smad signaling by Tob in osteoblasts. *Cell* **103**, 1085-1097.

Zhang, Y. W., Yasui, N., Ito, K., Huang, G., Fujii, M., Hanai, J., Nogami, H., Ochi, T., Miyazono, K. and Ito, Y. (2000). A RUNX2/PEBP2alpha A/CBFA1 mutation displaying impaired transactivation and Smad interaction in cleidocranial dysplasia. *Proc. Natl. Acad. Sci. USA* **97**, 10549-10554.

Journal of Cell Science

ELSEVIER

Bone 41 (2007) 543–548

BONE

www.elsevier.com/locate/bone

Prostaglandin E_2 EP4 agonist (ONO-4819) accelerates BMP-induced osteoblastic differentiation

Keisuke Nakagawa*, Yuuki Imai, Yoichi Ohta, Kunio Takaoka

Department of Orthopaedic Surgery, Osaka City University Graduate School of Medicine, Asahimachi 1-4-3, Abenoku, Osaka 545-8585, Japan

Received 12 May 2006; revised 3 June 2007; accepted 20 June 2007
Available online 29 June 2007

Abstract

Bone morphogenetic proteins (BMPs) were originally isolated based on their ability to induce ectopic cartilage and bone formation. The agents to promote the local bone formation with BMP would be beneficial to promote bone repair and to shorten the treatment period. For this purpose, we have examined ONO-4819, which is a prostaglandin (PG) E_2 EP4 receptor selective agonist (EP4A), as a positive modulators for the efficacy of BMPs. In our previous study, the systemic and local (with biodegradable synthetic polymers) administration of EP4A led to a significant augmentation of ossicle mass. But the mechanisms how EP4A accelerates the BMP-mediated bone formation are still unknown. In this study, we have examined how EP4A facilitates the BMP signaling using *in vitro* system with pluripotent stromal cell line, ST2. The mRNA expressions of Osterix and ALP (a marker enzyme of osteoblastic differentiation) and enzymatic activity of ALP in the ST2 cells were elevated significantly by BMP treatment. This elevation was further elevated by addition of the EP4A. The accelerated BMP action by the EP4A was abolished by pre-treatment with PKA inhibitor.

This study suggests that ONO-4819 accelerates BMP-induced osteoblastic differentiation of ST2 cells by stimulating the commitment for osteoblastic lineage. Thus PKA signaling pathway would be the main intracellular signaling pathway of the EP4 for the anabolic effect of bone and mineral metabolisms.

Keywords: Bone morphogenetic protein; Osteoprogenitor cells; Cyclic adenosine monophosphate; EP4 agonist

Introduction

Enhanced local new bone (callus) formation is an essential biological reaction during the repair of fractured or damaged bone. Agents that promote local bone formation would accelerate bone repair and shorten the treatment period. Prostaglandin E_2 (PGE_2) has been shown to promote bone formation both in *in vivo* [1] and *in vitro* [2] experimental systems. PGE_2 action is mediated through 4 types of prostaglandin E_2 receptors (EP1, EP2, EP3 and EP4) [3]. The osteogenic action of PGE_2 is mediated exclusively through EP4 in osteoblasts, based on the experimental evidence that PGE_2-mediated bone formation was abolished in EP4 knock-out mice but not in the EP1-, EP2- and EP3-knock-out mice [4]. The involvement of the EP4 receptor in the osteogenic action of PGE_2 was also shown through enhanced new bone formation following continuous exposure of osteoblasts to a selective EP4 agonist [5]. In our previous studies, we noted that elevation of intracellular cAMP by phosphodiesterase inhibitors (pentoxifylline and rolipram) and a permeable analogue of cAMP (dibutyril cAMP) enhanced BMP action and caused an increase in alkaline phosphatase activity of osteoblastic cells [6]. Additionally, in an experimental bone induction model, addition of the EP4 agonist to ectopic implants containing rhBMP-2 caused an increase in induced bone mass in a dose-dependent manner in mice [7]. In reviewing these data, it was hypothesized that elevated levels of cAMP might enhance BMP signaling at the transcriptional level. EP4 bound to ligand (PGE_2) mediated activation of adenylate cyclase by the α subunit of Gs protein ($G_s\alpha$) and subsequent activation of cyclic AMP-dependent protein kinase A (PKA) would phosphorylate the cAMP-responsive element binding protein (CREB) and thereby regulate the transcriptional function of CRE. However, it is not yet known to what extent the PKA

* Corresponding author. Fax: +81 6 6646 6260.
E-mail address: k-nakagawa@msic.med.osaka-cu.ac.jp (K. Nakagawa).

8756-3282/$ - see front matter © 2007 Elsevier Inc. All rights reserved.
doi:10.1016/j.bone.2007.06.013

signaling pathway interacts with BMP-mediated signaling to regulate osteoblastic differentiation.

The present paper describes the results of studies aimed at to elucidate 'cross-talk' between the EP4-mediated and BMPR-mediated intracellular signaling pathways to provide further insights into how PGE_2 promotes bone formation.

Materials and methods

Cell cultures

Murine bone marrow-derived stromal cells (ST2) and pluripotent mesenchymal cells (C2C12, C3H10T1/2) were obtained from the RIKEN Cell Bank (Tsukuba, Japan). Primary calvarial osteoblasts and myoblasts were obtained from an 18-day pc.fetus of ICR strain mice by enzymatic digestion. Cells obtained from these sources were seeded at a cell density of 3×10^5 cells per 100-mm plastic dish and cultured in α-minimal essential medium (α-MEM; Sigma, St. Louis, MO, USA) containing 10%(vol./vol.) or 2.5%, heat-inactivated fetal bovine serum (FBS; Gibco, Grand Island, NY, USA) at 37 °C in 5% CO_2 humidified air. Upon approaching confluency, the cells were harvested for use in specific experiments.

Reagents

Recombinant BMP-2 of human type (rhBMP-2) was produced by Wyeth Pharmaceutical Co. (Cambridge, MA) and donated to us through Astellas Pharmaceutical Co. (Tokyo, Japan). The rhBMP-2 was supplied in a buffer solution (5 mmol/l glutamic acid, 2.5% glycine, 0.5% sucrose, and 0.01% Tween-80) at a concentration of 3.52 μg/μl after filter sterilization. Prostaglandin E_2 was purchased from Sigma Chemical Co. (St. Louis, MO, USA). A synthetic selective EP4 receptor agonist (EP4A) ONO-4819, EP4 receptor antagonist ONO-3208, and an EP2 receptor agonist (EP2A) ONO-1259 were provided by Ono Pharmaceutical Co. (Osaka, Japan). The kinase inhibitors used were myristoylated PKI (Biomol Research Laboratories Inc.) for PKA, Gö-6976 (Calbiochem Co.) for PKC, SB203580 (Sigma Chemical Co.) for MAPK and LY294002 (Cayman Chemical Co.) for PI3K.

MTT assay

Cell viability was evaluated with an assay kit using MTT (3-[4,5-dimethylthyazol-2-yl]-2,5-diphenyl tetrazolium bromide) according to the manufacturer's instructions (Promega, Madison, WI, USA). The original form of this assay was described by Mossman [7]. MTT solutions were added to the cells in each well of a 96-well tissue culture plate and incubated for 4 h at 37 °C. After incubation, the Solubilization/Stop solution were added to each well and then mixed thoroughly. The absorbance of each mixture was measured on a microplate reader at a wavelength of 570 nm.

Routine cell counting was also performed under a microscope with use of a hemocytometer. Cells were seeded in 6-well plates and incubation was begun. At sequential time points, the cells were detached from plate by trypsin and stained by trypan blue to exclude dead cells before cell counting.

Assay of cAMP production

To confirm the action of the EP4A in elevating the intracellular cAMP level via EP4 receptor, the cAMP levels in ST2 cells stimulated with the EP4A alone or concurrently with rhBMP-2 (100 ng/ml) were measured and compared with control ST2 cells without treatment. After 20 min of pretreatment with 0.5 mM IBMX, cells were treated with rhBMP-2 and EP4A for 10 min. The medium was then removed and the level of cAMP determined using a cAMP enzyme immunoassay system (GE Healthcare).

Real-time reverse transcription polymerase chain reaction (RT–PCR)

The effects of EP4A on BMP-2-induced Osterix (OSX) and ALP (alkaline phosphatase) expressions were investigated quantitatively by real-time reverse transcriptase polymerase chain reaction (RT–PCR). When cultures maintained in 12-well plates ($n=3$ per group) became confluent, growth medium containing 2.5% FBS, rhBMP-2 and EP4A was added to the cultures. Total RNA was prepared from ST2 cells treated with each chemical for each time period (0, 3, 6, and 12 h, 1, 2, and 3 days) at 37 °C using NucleoSpin RNA II (Marchery-Nagel, Duren, Germany) according to the manufacturer's instructions. After cleaning of the isolated RNA using the RNeasy kit (Qiagen, Hilden, Germany), 5 μg of total RNA was reverse-transcribed into first-strand cDNA with an oligo-dT primer using Superscript II reverse transcriptase (Invitrogen, CA, USA). Real-time RT–PCR was performed using the vendor's protocols (Applied Biosystems, Foster City, CA, USA). Quantitative PCR analysis was performed using an iCycler apparatus (Bio-Rad laboratories, Hercules, CA, USA) and the iCycler Optical System Interface software (version 3.0; Bio-Rad). *Taq*Man fluorogenic probes for OSX, ALP and β-actin, an internal control, were purchased from Applied Biosystems (Foster City, CA, USA). Real-time RT–PCR was performed using Absolute QPCR low rox Mixs (Applied Biosystems, Foster City, CA, USA). Experimental samples were matched to a standard curve generated by amplifying serially diluted products using the same PCR protocol. To correct variability in RNA recovery and efficiency of reverse transcription, β-actin cDNA was amplified and quantified in each cDNA preparation. Normalization and calculation steps were performed as described by Pfaffl [8]. For the *in vitro* study, experiments were performed on three separate test occasions with an n of 3 for each test occasion.

Assay for alkaline phosphatase (ALP) activity

Alkaline phosphatase (ALP) levels in cells were assayed to evaluate osteoblastic differentiation levels under the influence of exogenous BMP and/or EP4A. Cells were seeded at a density of 1×10^4 cells/well in 48-well plates ($n=6$ per group). First, cells were treated with medium in the presence of 50 ng/ml of rhBMP-2 and various concentrations of EP4A (10^{-9} M to 10^{-5} M).

Following a review of the data from these experiments, a concentration of 10^{-7} M EP4A was used for the following series of studies. Cells were treated with medium in the presence or absence of 50 ng/ml of rhBMP-2 and/or 10^{-7} M of EP4A for 2 days with ST2 cells. The cells were washed twice with normal saline, solubilized with 0.2% Triton X in saline, frozen and then thawed. The cells were subsequently, sonicated in cold water and supernatants were measured for ALP activity as described previously [9] using *p*-nitrophenylphosphate as the substrate. One unit of activity is defined as 1 nmol *p*-nitrophenol liberation/30 min. Activity was normalized by protein content assayed with the Bio-Rad kit (BioRad) according to Lowry's method and expressed as a percentage of the control value in the absence of rhBMP-2 or EP4A. Independent experiments were performed in triplicate.

The effects of EP4A on rhBMP-2-induced ALP levels in primary osteoblasts and C2C12 cells were also investigated by treating those cells with 50 ng/ml of rhBMP-2 with or without concurrent treatment with EP4A for 6 days. After those treatments, the ALP levels in the different treatment groups were determined as described above. The respective mean level was determined from values in triplicate samples.

Effects of protein kinase inhibitors on the ALP activity

In order to identify the intracellular pathway of the EP4A-induced signaling on BMP action, specific inhibitors to PKA, protein kinase C (PKC), mitogen-activated protein kinase (MAPK) or phosphatidylinositol 3-kinase (PI3K) was used. ST2 cells were pre-treated with medium containing respective inhibitor for 15 min followed by rhBMP-2 (50 ng/ml) and EP4A (10^{-7} M) and incubated for a further 2 days. The effects of the inhibitors were estimated by measuring ALP levels as described above. The respective mean level was determined from values in triplicate sample.

Statistical analysis

Data were expressed as mean±SD for each group and analyzed by one-way analysis of variance (ANOVA) followed by Fisher's protected least significant difference (PLSD). Values of $p<0.05$ were considered to be significant.

Results

Cell viability

Cell viability as measured by MTT assay (Fig. 1) and cell counting (data not shown) showed no significant effect of BMP and EP4A treatment on the growth of cells examined until 7 days.

Elevation of intracellular cAMP levels by EP4A

In ST2 cells, cAMP levels increased significantly in 10 min of EP4A treatment (Fig. 2). No change in the intracellular cAMP level was recorded following treatment with rhBMP-2 alone and no additive cAMP elevation was noted by concurrent treatment with EP4A and rhBMP-2.

Effect of EP4A on osteoblastic differentiation induced by rhBMP-2

Fig. 3 indicates the effects of EP4A on the induction of ALP (early differentiation marker of osteoblasts) activity by rhBMP-2 in primary osteoblasts (Fig. 3a), C2C12 cells (Fig. 3b), ST2 cells (Fig. 3c), C3H10T1/2 cells and primary myoblasts cells (data not shown). All of these cells consistently responded to the rhBMP-2 and ALP levels were elevated. The addition of EP4A significantly and consistently enhanced the rhBMP-2-induced ALP activity. In ST2 cells, similar results were obtained when PGE_2 (10 nM) was added in place of EP4A (data not shown). In a further experiment, the enhancement of the rhBMP-2-induced ALP activity was abolished by the addition of an EP4 antagonist (Fig. 3c). The additional enhancement of BMP-induced ALP activity by EP4A was reproduced by the addition of dibutylyl cAMP [6].

Changes of rhBMP-2-induced Osterix and ALP expressions by the addition of the EP4 agonist

From the real-time RT-PCR analysis, Osterix and ALP mRNA expression were increased by rhBMP-2 treatment and further enhanced by EP4A addition (Fig. 4). These results

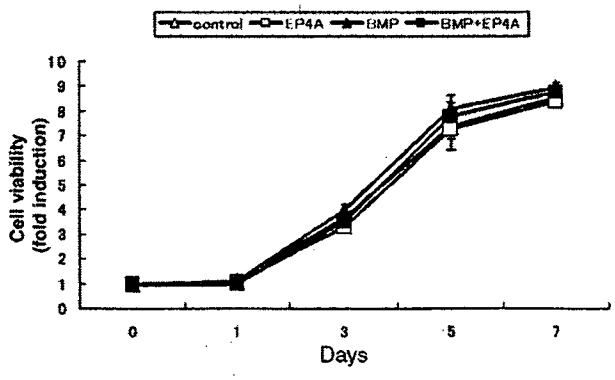

Fig. 1. Cell viability as measured by MTT assay. BMP and EP4A treatment showed no significant effect on the growth of cells examined until 7 days. Bars and lines represent mean±SD for 4 wells.

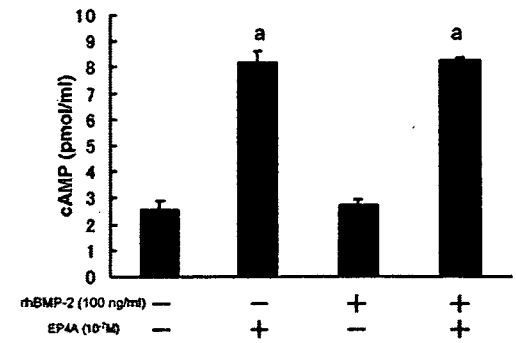

Fig. 2. Effects of EP4A on intracellular cAMP production in 10 min. ST2 cells were pre-incubated in α-MEM, then incubated with 50 ng/ml of rhBMP-2 and/or 10^{-7} M of EP4A. Intracellular cAMP levels of the cells treated with EP4A were significantly elevated. Bars and lines represent mean±SD for 4 wells. $^{a}p<0.01$ to the group treated without EP4A and rhBMP-2.

indicated that the EP4A potentially enhanced the rhBMP-2 action at a mRNA level in early phase.

Intracellular signaling pathway involved in the EP4A action on BMP signaling

In order to investigate intracellular signaling pathway involved in the mechanism to enhance BMP signaling by EP4A, the effects of kinase inhibitors were examined. As shown in Fig. 5, the inhibitors against PKC (Gö-6976) (Fig. 5a), MAPK (SB203580) (Fig. 5b) and PI3K (LY294002) (Fig. 5c) did not inhibit the EP4A-induced additional elevation of rhBMP-2-induced ALP activity. Only a PKA inhibitor (myristoylated PKI) (Fig. 5d) abolished the EP4A action completely. We concluded that the action of the EP4A was mediated via the PKA signaling pathway.

Discussion

A few studies have revealed close relationships of PGE_2 and PGE_2-producing enzymes such as COX-2 or PGE synthase with biological action of BMP. One study [10] indicated that COX-2 expression might be increased by BMP-2 stimulation to osteogenic cells via core-binding factor activity 1 (Cbfa1/Runx2) binding to its consensus sequence in the COX-2 promoter region, and that BMP-induced osteoblastic differentiation was dramatically reduced in COX-2 knock-out mice. Another study [11] revealed suppression of expression of BMP-2 by COX-2 inhibitor, in human mesenchymal stem cells, suggesting the possible involvement of PGE_2 in regulation of BMP-2 expression. In addition to these findings, the present study indicated that exogenously administered EP4 agonist (an analogue of PGE_2) enhanced the biological effects of BMP-2. The previous and present experimental findings suggest the presence of co-operative or auto-regulatory mechanisms between BMP-2 and PGE_2 signaling systems in maintaining or promoting osteoblastic differentiation of cells with osteogenic potential.

The enhancement of BMP action by an EP4A might also be driven by the increased intracellular accumulation of cAMP

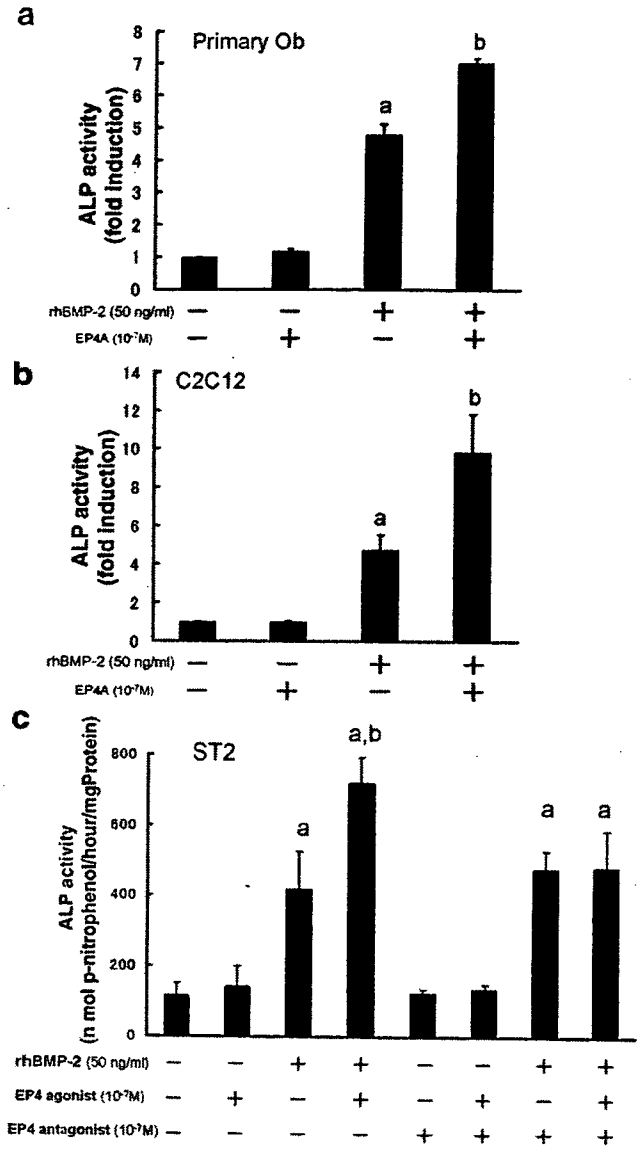

Fig. 3. Effects of EP4A on osteoblastic differentiation induced by rhBMP-2. Alkaline phosphatase (ALP) activities were assayed to evaluate the effects of BMP, EP4agonist and EP4antagonist on osteoblastic differentiation. The results of ALP activities of primary osteoblasts (a), C2C12 cells (b) and ST2 cells (c) treated with or without 50 ng/ml of BMP-2 and/or 10^{-7} M of EP4A are shown. ALP activities of all cells treated with both of BMP-2 and EP4A were increased when compared to that of all cells treated with BMP-2 only. The effects of EP4A were abolished by the addition of the EP4 antagonist (c). Bars and lines represent mean ± SD for 4 wells. $^{a}p<0.05$ to the group treated without EP4A and rhBMP-2, $^{b}p<0.05$ to the group treated with rhBMP-2 alone.

based on data from previous *in vivo* [12] and *in vitro* [13] studies. Relationship between intracellular cAMP concentration and intracellular BMP signaling has not been clarified. EP4A alone could not elicit ALP induction, but it enhanced BMP-induced ALP induction as shown in Fig. 3. The rhBMP-2-dependent action of EP4A was also noted in BMP-induced Osterix and ALP expression (Fig. 4). One of the possible intracellular events subsequent to cAMP accumulation would be the activation of cAMP-dependent kinase PKA, since the effect of EP4A was abolished by a PKA-specific inhibitor (myristoylated PKI) (Fig. 5d). Activated PKA phosphorylates cAMP responsive element binding protein (CREB) to regulate CRE-dependent gene expression [14]. A similar effect of EP4A was observed during the formation of ectopic new bone mass in the muscles following the implantation of rhBMP-2 containing collagen pellets [12,15,16]. These compounds also enhanced BMP-induced ALP expression *in vitro* [6,13].

It was reported that systemic administration of an EP4 agonist (ONO-4819) enhanced new bone formation and prevented bone loss by unloading or ovariectomy in mice [17,18], and an EP4 antagonist suppressed bone formation induced by PGE_2 [19]. Following the reports, we previously reported that systemic [20] and local (with biodegradable synthetic polymers) [7] administration of the EP4A led to the significant augmentation of size and bone mineral density of ectopic ossicles induced by rhBMP-2. At that time, it was equivocal whether EP4A stimulated the BMP signaling or the growth of osteoblastic cells induced by BMP. The results from the present study would indicate that EP4A enhanced BMP signaling at mRNA level to promote the osteoblastic differentiation process.

Effects of protein kinase inhibitors of PKA, protein kinase C (PKC), mitogen-activated protein kinase (MAPK) and phosphatidylinositol 3-kinase (PI3K), showed that the anabolic

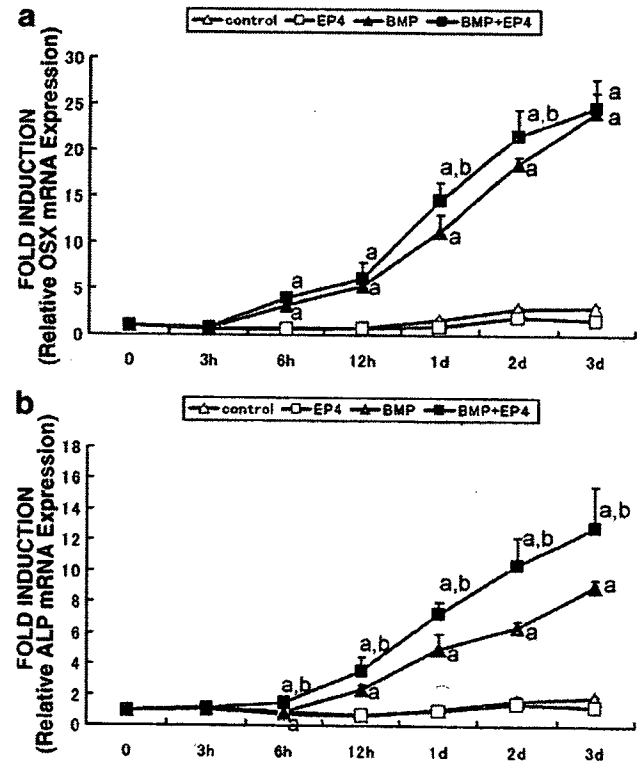

Fig. 4. Relative expression of mRNA for Osterix (a) and ALP (b). Total RNA was prepared from ST2 cells treated with or without BMP and EP4A for each time period (0, 3, 6, and 12 h, 1, 2 and 3 days) on the 12-well plate. Relative mRNA expression was normalized using amplified B-actin expression values. The mRNA expression of Osterix and ALP was increased by rhBMP-2 treatment and further enhanced by EP4A addition. In day 3, Osterix mRNA expression levels were equal in BMP group and BMP/EP4A group. Bars and lines represent mean ± SD for 4 wells. $^{a}p<0.05$ to the group treated without EP4A and rhBMP-2, $^{b}p<0.05$ to the group treated with rhBMP-2 alone.

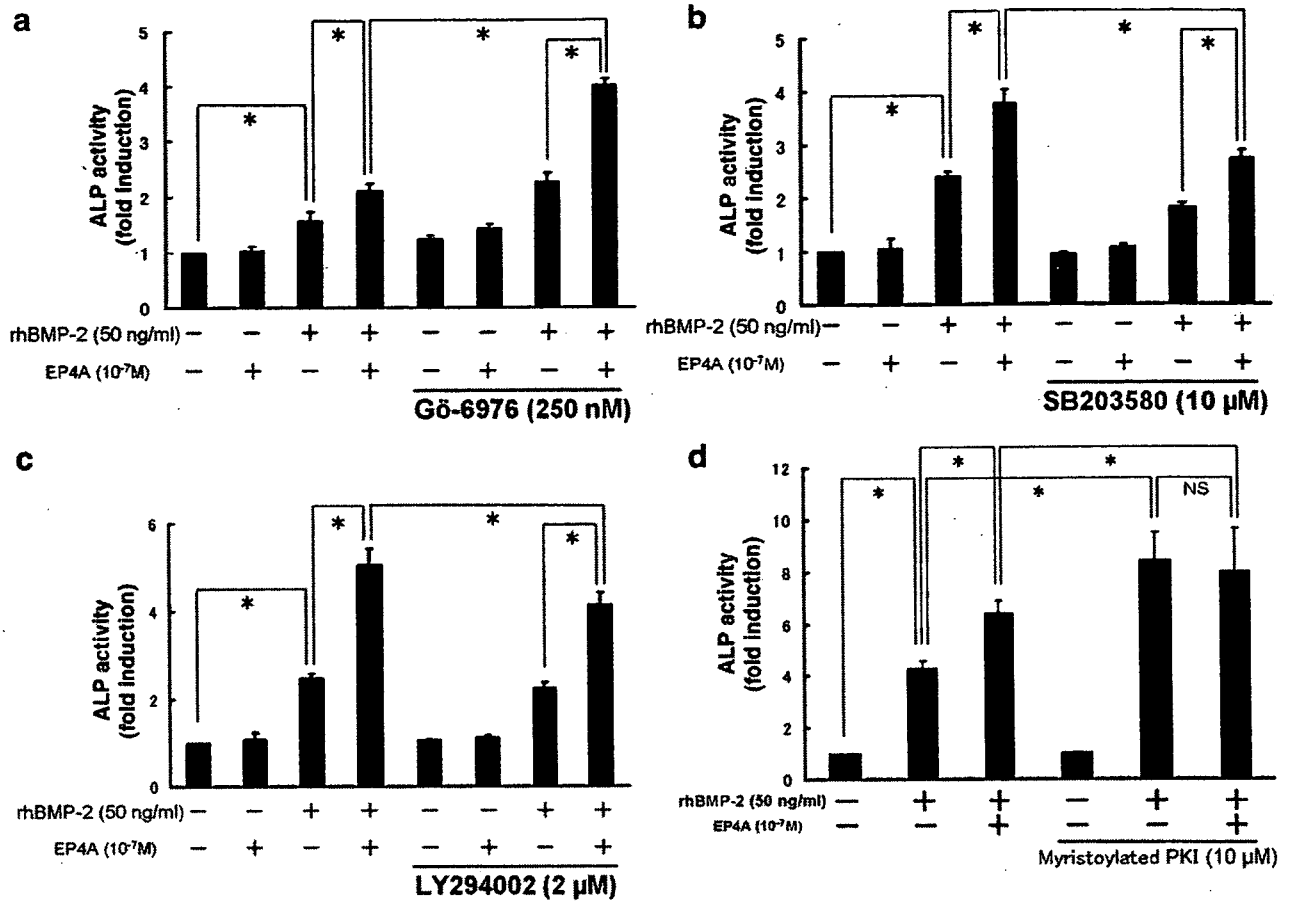

Fig. 5. Effects of protein kinase inhibitors on BMP induced osteoblastic differentiation enhanced with the EP4A. Alkaline phosphatase (ALP) was used as a marker to evaluate the effects of BMP-2, EP4A and respective protein kinase inhibitors on osteoblastic differentiation. Cells were pre-treated with medium containing one of the inhibitors for 15 min before treatment. 250 nM Gö-6976 for PKC inhibitor (a), 10 μM SB203580 for MAPK inhibitor (b), 2 μM LY294002 for PI3K inhibitor (c) and 10 μM myristoylated PKI for PKA inhibitor (d) were used to inhibit respective protein kinases. The value of control group was indicated as 1. Enhancement of BMP induced osteoblastic differentiation by EP4A was abolished by the PKA inhibitor. Bars and lines represent mean ± SD for 4 wells. $^{a}p<0.05$ to the group treated without EP4A and rhBMP-2, $^{b}p<0.05$ to the group treated with rhBMP-2 only, $^{c}p<0.05$ to the group treated with EP4A and rhBMP-2, $^{*}p<0.05$.

effect of EP4A might be mediated via the PKA signaling pathway. However, it appeared curious that pretreatment by myristoylated PKI alone increased responsiveness to BMP. Although the reason of the increased responsiveness to BMP by inhibition of PKA could not be identified in this study, but one possible explanation might be the presence of unknown suppressive regulatory mechanism to BMP action involving PKA. Considering other protein kinases, MAPK and PI3K inhibitors blocked the effect of EP4A only partially. PKC inhibitor, on the other hand, enhanced the effects of BMP and EP4A. The mechanism by which PKC inhibitor enhances the effects of BMP and EP4A was not clarified. One possibility is that PKC kinase is involved in dephosphorylation of ATP to ADP, and that PKC inhibitor preserves ATP, which would be metabolized to cAMP by adenylyl cyclase. This is only a hypothesis and further study is needed to clearly determine the mechanism.

Currently, certain BMP molecules (BMP-2, BMP-7) with a dimeric molecular structure are produced commercially in CHO cells by DNA recombination technology with low efficiency [21]. In considering the clinical use of BMP to promote the regenerative repair of fractures or bone defects, several problems need to be addressed. A major challenge is the high cost of the BMP due to the low responsiveness of humans to this protein. The result is a requirement for high doses of BMP and consequent high cost for production of this protein in CHO cells. In this context, any method that enhances the efficacy of BMPs and reduces the cost of BMP-retained implants warrants further exploration. From a clinical perspective, the EP4A used in this study (ONO-4819) could be a promising agent for bone formation because it consistently enhanced BMP activity and induced more bone when compared to BMP alone [7].

Acknowledgments

This work was supported in part by a Grant-in-Aid from the Ministry of Education, Culture, Sports, Science and Technology of Japan (Project Grant No. 30112048, 17591588, 17591589, 17659477, 18390421, 18591640). The authors thank members of Central Laboratory of Osaka City University Graduate School of Medicine for cooperation in this

References

[1] Weinreb M, Suponitzky I, Keila S. Systemic administration of an anabolic dose of PGE_2 in young rats increases the osteogenic capacity of bone marrow. Bone 1997;20:521–6.

[2] Keila S, Kelner A, Weinreb M. Systemic prostaglandin E_2 increases cancellous bone formation and mass in aging rats and stimulates their bone marrow osteogenic capacity in vivo and in vitro. J Endocrinol 2001;168: 131–9.

[3] Suda M, Tanaka K, Natsui K, Usui T, Tanaka I, Fukushima M, et al. Prostaglandin E receptor subtypes in mouse osteoblastic cell line. Endocrinology 1996;137:1698–705.

[4] Yoshida K, Oida H, Kobayashi T, Maruyama T, Tanaka M, Katayama T, et al. Stimulation of bone formation and prevention of bone loss by prostaglandin E EP4 receptor activation. Proc Natl Acad Sci U S A 2002;99:4580–5.

[5] Machwate M, Harada S, Leu CT, Seedor G, Labelle M, Gallant M, et al. Prostaglandin receptor EP(4) mediates the bone anabolic effects of PGE (2). Mol Pharmacol 2001;60:36–41.

[6] Sugama R, Koike T, Imai Y, Nomura-Furuwatari C, Takaoka K. Bone morphogenetic protein activities are enhanced by 3′,5′-cyclic adenosine monophosphate through suppression of Smad6 expression in osteoprogenitor cells. Bone 2006;38:206–14.

[7] Toyoda H, Terai H, Sasaoka R, Oda K, Takaoka K. Augmentation of bone morphogenetic protein-induced bone mass by local delivery of a prostaglandin E EP4 receptor agonist. Bone 2005;37:555–62.

[8] Pfaffl MW. A new mathematical model for relative quantification in real-time RT–PCR. Nucleic Acids Res 2001;29:e45.

[9] Imai Y, Terai H, Nomura-Furuwatari C, Mizuno S, Matsumoto K, Nakamura T, et al. Hepatocyte growth factor contributes to fracture repair by upregulating the expression of BMP receptors. J Bone Miner Res 2005; 20:1723–30.

[10] Chikazu D, Li X, Kawaguchi H, Sakuma Y, Voznesensky OS, Adams DJ, et al. Bone morphogenetic protein 2 induced cyclo-oxygenase 2 in osteoblasts via a Cbfa1 binding site: role in effects of bone morphogenetic protein 2 in vitro and in vivo. J Bone Miner Res 2002;17:1430–40.

[11] Arikawa T, Omura K, Morita I. Regulation of bone morphogenetic protein-2 expression by endogenous prostaglandin E_2 in human mesenchymal stem cells. J Cell Physiol 2004;200:400–6.

[12] Horiuchi H, Saito N, Kinoshita T, Wakabayashi S, Yotsumoto N, Takaoka K. Effect of phosphodiesterase inhibitor-4, rolipram, on new bone formations by recombinant human bone morphogenetic protein-2. Bone 2002;30:589–93.

[13] Tsutsumimoto T, Wakabayashi S, Kinoshita T, Horiuchi H, Takaoka K. A phosphodiesterase inhibitor, pentoxifylline, enhances the bone morphogenetic protein-4 (BMP-4)-dependent differentiation of osteoprogenitor cells. Bone 2002;31:396–401.

[14] Shaywitz AJ, Greenberg ME. CREB: a stimulus-induced transcription factor activated by a diverse array of extracellular signals. Annu Rev Biochem 1999;68:821–61.

[15] Horiuchi H, Saito N, Kinoshita T, Wakabayashi S, Tsutsumimoto T, Takaoka K. Enhancement of bone morphogenetic protein-2-induced new bone formation in mice by the phosphodiesterase inhibitor pentoxifylline. Bone 2001;28:290–4.

[16] Horiuchi H, Saito N, Kinoshita T, Wakabayashi S, Tsutsumimoto T, Otsuru S, et al. Enhancement of recombinant human bone morphogenetic protein-2 (rhBMP-2)-induced new bone formation by concurrent treatment with parathyroid hormone and a phosphodiesterase inhibitor, pentoxifylline. J Bone Miner Metab 2004;22:329–34.

[17] Hayashi K, Fotovati A, Ali SA, Oda K, Oida H, Naito M. Prostaglandin EP4 receptor agonist augments fixation of hydroxyapatite-coated implants in a rat model of osteoporosis. J Bone Jt Surg Br 2005;87:1150–6.

[18] Tanaka M, Sakai A, Uchida S, Tanaka S, Nagashima M, Katayama T, et al. Prostaglandin E_2 receptor (EP4) selective agonist (ONO-4819.CD) accelerates bone repair of femoral cortex after drill-hole injury associated with local upregulation of bone turnover in mature rats. Bone 2004;34: 940–8.

[19] Shamir D, Keila S, Weinreb M. A selective EP4 receptor antagonist abrogates the stimulation of osteoblast recruitment from bone marrow stromal cells by prostaglandin E_2 in vivo and in vitro. Bone 2004;34: 157–62.

[20] Sasaoka R, Terai H, Toyoda H, Imai Y, Sugama R, Takaoka K. A prostanoid receptor EP4 agonist enhances ectopic bone formation induced by recombinant human bone morphogenetic protein-2. Biochem Biophys Res Commun 2004;318:704–9.

[21] Sampath TK, Maliakal JC, Hauschka PV, Jones WK, Sasak H, Tucker RF, et al. Recombinant human osteogenic protein-1 (hOP-1) induces new bone formation in vivo with a specific activity comparable with natural bovine osteogenic protein and stimulates osteoblast proliferation and differentiation in vitro. J Biol Chem 1992;267:20352–62.

Repair of Bone Defects in Revision Hip Arthroplasty by Implantation of a New Bone-Inducing Material Comprised of Recombinant Human BMP-2, Beta-TCP Powder, and a Biodegradable Polymer: An Experimental Study in Dogs

Masatoshi Hoshino, Takashi Namikawa, Minori Kato, Hidetomi Terai, Susumu Taguchi, Kunio Takaoka

Department of Orthopedic Surgery, Osaka City University Graduate School of Medicine, 1-4-3 Asahi-Machi Abeno-Ku Osaka, 545-8585 Japan

Received 30 October 2006; accepted 19 March 2007

Published online 27 April 2007 in Wiley InterScience (www.interscience.wiley.com). DOI 10.1002/jor.20424

ABSTRACT: A recombinant BMP-2-retaining putty-form implant in combination with a hip prosthesis was used to reconstruct a canine hip joint with defects similar to those encountered in revision total hip arthroplasty (THA). The bone defects were made by resecting the medial half of the proximal femur and the superior acetabular bone with inner iliac wall perforation in 10 dogs. In five dogs, hip prostheses were implanted with the putty material consisting of a synthetic polymer (poly D,L-lactic acid-polyethylene glycol block copolymer), β-tricalcium phosphate powder, and recombinant human BMP-2 in each defect (BMP/Polymer/TCP group). In the remaining five dogs, the same material without rhBMP-2 (control group) was implanted. In the BMP/Polymer/TCP group, new radiopaque shadows began to appear 4 weeks after surgery at the defects around the hip prostheses on both the femoral and acetabular sides. At 12 weeks, the defects were completely filled with new bone in contact with the prosthesis. On histology, the rhBMP-2/Polymer/β-TCP composite putty implants had been completely resorbed and replaced by new bone. Repair of the bone defects was not seen in the control group. The ability of this material to restore bone effectively eliminates the dependency on bone grafts of autogeneic or allogeneic origin for revision hip arthroplasty and thus opens up a potential new treatment approach in hip cases requiring this type of surgery. © 2007 Orthopaedic Research Society. Published by Wiley Periodicals, Inc. J Orthop Res 25:1042–1051, 2007

Keywords: bone defects; BMP/Polymer/TCP group; dogs

INTRODUCTION

Currently, total hip arthroplasty (THA) is a standard treatment of hip disorders associated with significant disability. Globally, large numbers of patients have undergone THA, and satisfactory long-term clinical outcomes have been reported without complications in the early postoperative phase.[1–6] Satisfactory hip function is maintained as long as the prosthesis remains firmly fixed to the host bone. However, over time, layers of fibrous tissue are generated at the interface between the host bone and prosthesis (with cementless fixation) or cement mantle (with cement fixation). This is likely due to migration of polyethylene wear particles into the interface, resulting in chronic inflammation, bone resorption, and loosening of the prosthesis and leading to hip and thigh pain and increasing dysfunction of the joint.[7–9]

Fibrous tissue growth routinely associates with periprosthetic osteolysis, and bone defects of varying size are encountered at revision surgery. This causes difficulty in securing fixation of a new prosthesis; the extent of the problem depends on the severity of the bone defects. When the defects are limited in size, specific modifications of the revision prosthesis (e.g., large-sized cementless metal acetabular sockets and long calcar replacement femoral stems) can solve the problem.[10–13] However, when the defects are large, augmentation with or without allo- or autogenetic bone graft or bone graft substitutes such as hydroxyapatite and tricalcium phosphate are needed to repair the defects. In these situations, fixation of the revision prosthesis is much more difficult.[14–17] Options for treatment include use of impaction morselized allograft and cement fixation of the prosthesis or the use of bulky allografts to fill the bone defect. Unfortunately, the latter approach comes with the risk for infection, limited sources of graft material, and limited osteogenic potential.[14,18,19]

Correspondence to: M. Hoshino (Telephone: +81-6-6645-3851; Fax: +81-6-6646-6260;
E-mail: hirotoy@msic.med.osaka-cu.ac.jp)

Revision surgery would be greatly enhanced if new methods were available to enhance bone regeneration and ultimately repair the defect without the use of bone grafts. One approach would be to utilize bone-inducing proteins (BMPs) in combination with an appropriate delivery system. Human BMP-2 and BMP-7 have osteoinductive capacities and are currently produced commercially by DNA recombination techniques (rhBMP-2, rhBMP-7).[20–23] The rhBMPs are used for spinal fusion, repair of nonunion fractures, and treatment of open tibial fractures using animal-derived collagen as a carrier material.[24–27]

To investigate the use of rhBMP to regenerate lost bone in hip revision surgery, we obtained a hip prosthesis for beagles and specially formulated BMP-retaining putty-form biodegradable materials to fill bone defects created in both the femur and acetabulum. The bone regeneration process was monitored by serial radiographs and computed tomography. The quality of the new bone was investigated using undecalcified histological sections.

MATERIALS AND METHODS

RhBMP-2 was produced by Wyeth (Cambridge, MA) and donated to us through Astellas Pharma Inc. (Tokyo, Japan), supplied in a buffered solution (5 mmol/L glutamic acid, 2.5% glycine, 0.5% sucrose, and 0.01% Tween-80) at a concentration of 3.52 μg/μL after filter sterilization. Poly-D, L-lactic acid-polyethylene glycol block copolymer (PLA-PEG) (MW; 9100, PLA/PEG molar ratio; LA/EO = 60/40), was synthesized and provided to us by Taki Chemical Co., Ltd. (Kakogawa, Japan). Details of the physicochemical characteristics of this biodegradable polymer were reported previously.[28–30] Beta-TCP powder (particle size <100 μm in diameter) was provided to us by Olympus Biomaterial Corp. (Tokyo, Japan).

To prepare an implant for one dog, 400 mg of β-TCP powder, 400 mg of PLA-PEG, and 200 μg of rhBMP-2 were stirred with a metal rod at 50°C for several minutes. The resultant dough was stored at −30°C until implantation. Control implants consisting of 400 mg of β-TCP powder and 400 mg of PLA-PEG but without rhBMP-2 were prepared in the same manner.

The acetabular and femoral prostheses were fabricated by Zimmer Japan Co., Ltd. (Tokyo, Japan). The titanium femoral stem was 65 mm long and 5 mm wide, with a varus inclination of 10°. Pure titanium fiber coarse metal mesh was diffusion-bonded to the proximal medial 25 mm of the stem. The ultrahigh molecular weight polyethylene head was 10 mm in diameter. The acetabular component had an outer diameter of 20 mm and a hemispherical shell covered with coarse pure titanium fiber mesh. Three small flanges with three screw holes at the periphery provided fixation to the anterior and posterior parts of the acetabular rim. The porous surfaces were covered manually with rhBMP-2/Polymer/β-TCP or Polymer/β-TCP composite or control at the time of surgery (Fig. 1a).

Ten Beagle dogs (male, 8 months old, weight, 9–11 kg) were purchased from Oriental Yeast Co., Ltd. (Tokyo, Japan) and fed in separate cages with free access to food and water. This animal study was approved by the Animal Care and Oversight Committee of Osaka City University Medical School. The animals were randomly divided into two groups (BMP/Polymer/TCP and Polymer/TCP group), five animals in each group.

Each animal was anesthetized by an intramuscular injection of ketamine (10 mg/kg) and xylazine (1.2 mg/kg) and maintained under anesthesia by an intravenous injection of pentobarbital (25 mg/kg). The right hip was exposed through an anterolateral approach by standard sterile techniques. After an anterior capsulotomy and section of the ligamentum teres, the hip was dislocated, and the femoral head and medial half of the proximal femoral (2.5 cm in length) were resected with an oscillating saw to create a bone defect. The acetabular floor cartilage and bone were then removed with a reamer (2-cm diam) up to the inner wall of the iliac bone, and the central part of the exposed inner wall was perforated (8-mm diam) with a high-speed air drill. In addition, a superior portion of the iliac bone including the superior acetabular rim (15 mm wide, 15 mm long, and 10 mm deep) was removed with a high-speed air drill. Figure 1b shows canine femoral and acetabular specimens with simulated bone defects. The acetabular component was then implanted with one-quarter of the rhBMP-2/Polymer/β-TCP or Polymer/β-TCP composite (control) and fixed to the remaining acetabular rim with titanium screws through the holes in the component flanges. The defect between the acetabular component and iliac bone was packed with one-quarter of the putty implant mass. The distal part of the stem was fixed with cement (Surgical Simplex P, London, England) into the femoral canal. The surface of the femoral component exposed to the proximal medial part was covered with the remaining putty material. After these procedures, the hip was reduced and the wound was closed. Care was taken so that the bone-defect sites were covered and in contact with muscles to keep the putty implant in place. Intra- and postoperative health of the animals was monitored carefully, and prophylactic antibiotics (10 mg/body weight) were administered once a day for 3 days after surgery.

Plain radiographs and CT scans were taken immediately after surgery and serially at 4-week intervals thereafter to monitor new bone formation at the defects. Twelve weeks after surgery, all animals were euthanized by overdose anesthesia, and the pelves and femurs containing the hip prosthesis were harvested. All dissected samples were examined by plain radiographs and CT scans and then fixed in 70% ethanol for histological examination. CT data of harvested acetabulum and femora were obtained with a helical CT

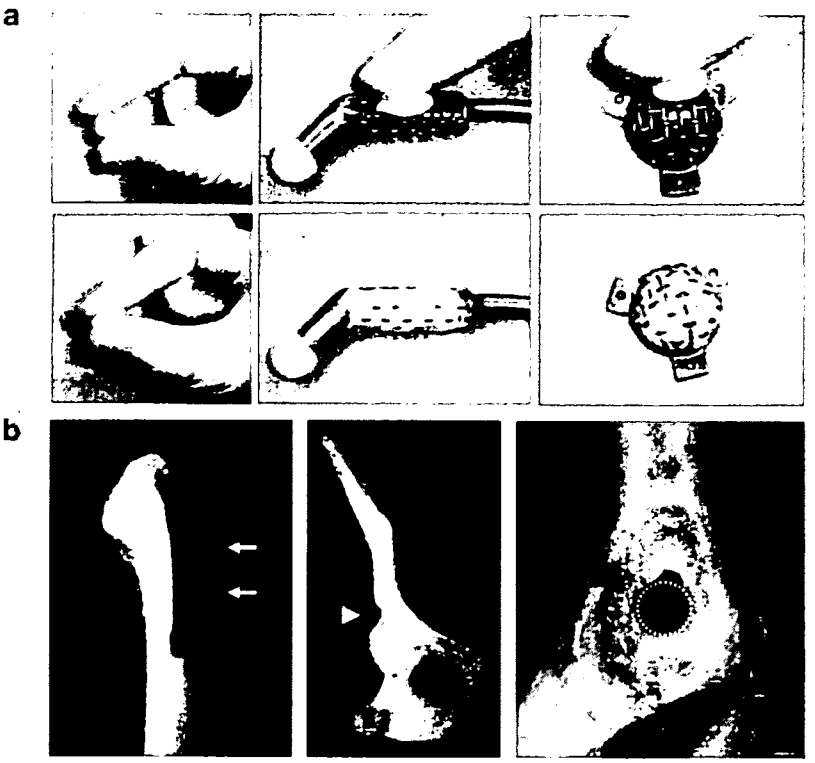

Figure 1. (a) Gross appearance of a new bone-inducing putty material comprised of β-TCP powder, PLA-PEG polymer, and rhBMP-2. (Left) The putty material can be molded at surgery. (Middle and right) The material was pushed manually into the mesh on the hip prosthesis. (b) Gross appearance of canine femoral and acetabular specimens with simulated bone defects. (Left) The defect in proximal femur was made by resecting the femoral head and medial half of the proximal femur (2.5 cm in length) (arrows). (Middle and right) Acetabular defects were created by resecting the superior acetabular bone (15 mm in width, 5 mm in length, and 10 mm in depth) and by perforating the medial wall of the acetabulum (8 mm in diameter) (arrow head and areas surrounded by dot lines).

(GE Yokogawa, Tokyo, Japan) with 1-mm slice thickness and were reconstructed to 3D images and frontal slice images with reconstruction soft-ware (Aze, Tokyo, Japan).

Soft tissues were removed and the samples soaked in Villanueva mineralized bone stain for 7 days, dehydrated in ascending grades of ethanol, defatted in an acetone/methylmethacrylate monomer (mixture rate: 1:2), and embedded in methylmethacrylate (Wako Chemicals, Kanagawa, Japan) without decalcification. Serial sections 200 μm thick were cut with a precision bone saw in a vertical direction for the central part of the acetabulum and a transverse direction at the femoral defect for the proximal femur. Sections were mounted on plastic slides and ground to 50 μm using a precision lapping machine (Maruto, Tokyo, Japan).

Quantification of new bone formation at the defects was made from reslice images obtained with the 3D CT images in a center plane at the acetabular defect and perpendicular to the femoral axis at the middle of the femoral defects. The mid reslice images and two 2-mm additional slices were measured at the defects in each dog. The new bone area including intertrabecular spaces was measured using Scion Image soft ware (Scion Corp., Frederick, MA). The average value of three new bone areas was expressed as new bone area (mm^2).

Mann-Whitney's *U*-test was used to determine significant differences with at $p < 0.05$.

RESULTS

All surgeries were completed successfully, and animals survived without any complications. The animals presented mild lameness immediately after surgery but recovered normal ambulation within 2–3 weeks.

Figure 2a shows time sequence changes in acetabular bone defects in experimental and control groups of dogs on reconstructed frontal CT slices. In the BMP/Polymer/TCP group animal, radiopaque shadows were noted in the superior and

DOI 10.1002/jor

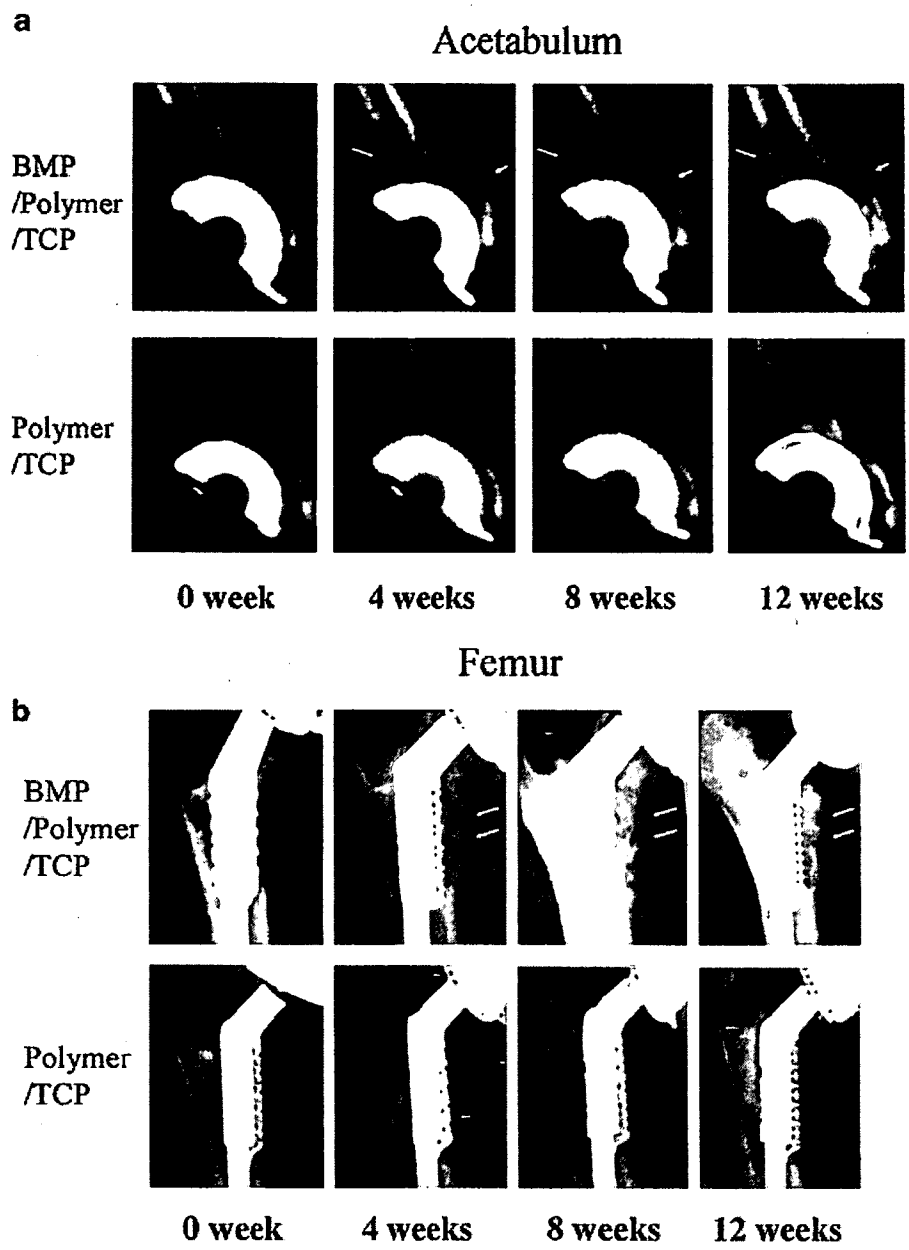

Figure 2. (a) Representative sequential reconstructed CT images of acetabular bone and (b) plain serial radiographs of the femoral bone defect are shown. The defects in the above column were implanted with the rhBMP-2/Polymer/β-TCP composite; the control defects shown in the lower column were implanted with Polymer/b-TCP composite. Arrows indicate new bone formed at the superior and medial wall defects of the acetabulum and along the prosthesis at the femoral defects at 4, 8, and 12 weeks after implantation in the BMP/Polymer/TCP group. No bone formation was noted on the control defects where Polymer/β-TCP composite was implanted.

medial acetabular wall defects at 4 weeks. At 8 weeks, the radiopaque mass in the defect became larger and more evident, and at 12 weeks the defects appeared fully repaired with evidence of remodeling and cortical bone formation. No loosening of the acetabular component was noted. Radiopaque shadows were not seen throughout the 12 week period in the control group.

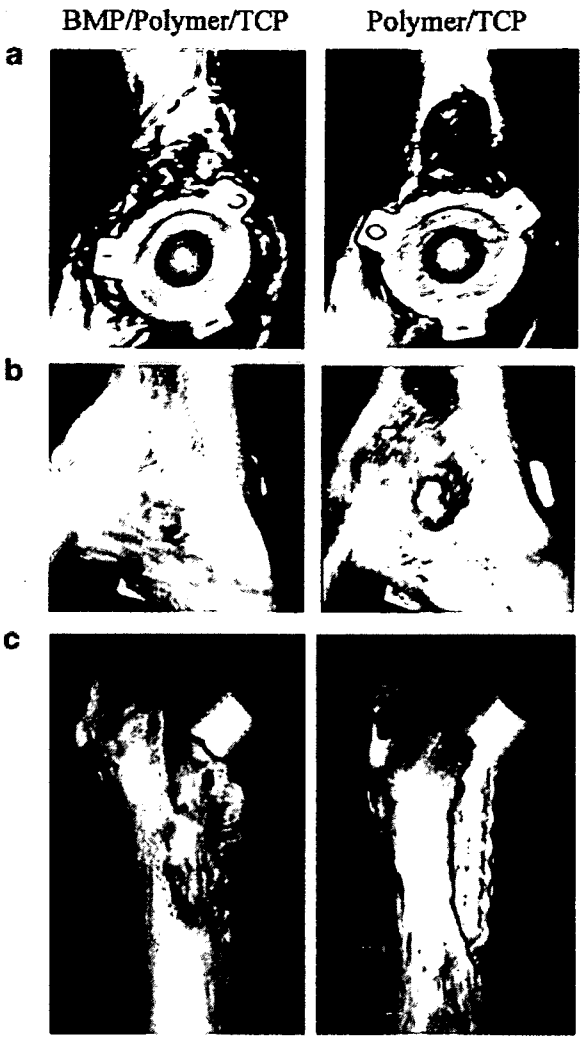

Figure 3. Representative 3D images of acetabular and femoral bones implanted with rhBMP-2/Polymer/β-TCP composite or Polymer/β-TCP composite and harvested 12 weeks after surgery. Bone defects in (a) the superior and (b) the medial acetabular wall and in (c) the proximal medial portion of femur were repaired by implanting the rhBMP-2 retaining putty.

On serial plain radiographs of the femoral defect, a pattern of repair similar to that seen in the acetabular defects was observed. At 4 weeks, speckles of radiopaque shadows were noted at the defects in parallel to the femoral implant in the BMP/Polymer/TCP group (Fig. 2b). At 8 weeks, a more dense radiopaque mass was seen around the implants at the defect. Twelve weeks after implantation, all implants in the BMP/Polymer/TCP group showed new bone formation at the defects. In the control group, no evidence of radiopaque deposits was seen, although a small amount of new bone was seen at distal cut ends of the defects. No further evidence of repair was noted throughout the 12 week period.

Repair of the bone defects was also confirmed in the samples from the BMP/Polymer/TCP group animal on the 3D CT images of the acetabulum and femur samples retrieved at 12 weeks (Fig. 3). In the control group, the defect of femoral implant remained unrepaired with no evidence of new bone formation.

Figure 4 shows representative undecalcified sections of the acetabulum and femur from an experimental BMP/Polymer/TCP group animal and a control group animal. In the BMP/Polymer/TCP group, the periacetabular bone defect and perforated hole at the medial iliac wall was occupied by a significant amount of new woven bone with fibrous tissue in the marrow space (Fig. 4c). Additionally, the new bone ingrowth onto the surface of the acetabular component was noted. In the control section, the defect as well as the perforated medial wall showed no signs of repair or ingrowth of bone onto the acetabular component, with no apparent loosening of the acetabular socket. The putty implant mass was not recognized on the section at 12 weeks after surgery. Inflammatory and foreign body reactions were not elicited by the implanted material at 12 weeks after surgery. The femoral bone defect was also repaired by a significant amount of new bone in the BMP/Polymer/TCP group. Ingrowth of the new bone on the femoral component surface was noted. In the control section, the defect was left unrepaired with no ingrowth of bone onto the femoral component. In BMP-treated defects, new bone formation was also observed within the titanium mesh of both acetabular and femoral components in contact with the titanium surface (Fig. 5). In the control group, fibrous tissue was observed predominantly at the defect site.

The BMP/Polymer/TCP group showed a time-dependent increase in new bone both in the acetabular and femoral defects, but the Polymer/TCP group showed only small areas of new bone formation through the experimental period (Fig. 6). The new bone area of the BMP/Polymer/TCP group at 4, 8, and 12 weeks was significantly higher than that of the Polymer/TCP group in both the acetabulum and femur.

DISCUSSION

Our experimental results indicate that bone defects in revision hip surgery can be repaired with the use of BMP in combination with a

DOI 10.1002/jor

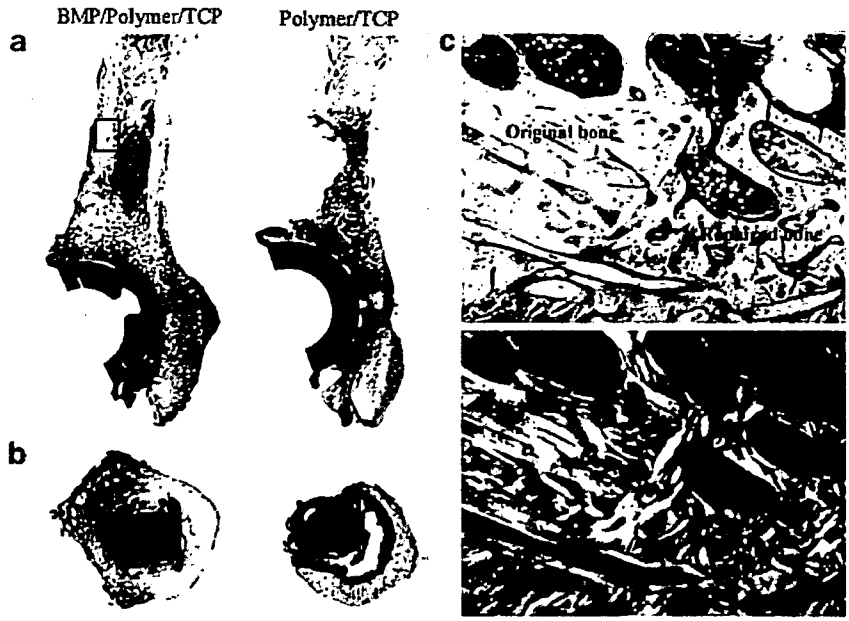

Figure 4. (a,b) Representative undecalcified sections (Villaneuva bone stain, ×2) of acetabular (a) and femoral (b) bone harvested 12 weeks after implantation. Sections on the left are from a dog implanted with rhBMP-2/Polymer/β-TCP composite and the right from control dogs implanted with the Polymer/β-TCP composite. In the BMP/Polymer/TCP dog, the defects showed complete repair. (c) Undecalcified histology at the junction area of the original bone and newly formed bone indicated by a rectangle in (a) (Villaneuva bone stain, ×50). The lower section shows the same microscopic field as that seen in the upper right panel, but under polarized light, indicating the woven structure of the newly formed bone.

delivery system. The defects generated in the acetabulum and proximal femurs would likely be classified as moderately severe (type III in AAOS classification for acetabular bone defects, and type I for proximal femoral defects), and clinically would require bone grafting and/or implantation of bone-graft substitutes with a significantly long postoperative period to restore hip function.[31,32] The key points to draw from our study are that: large bone defects were regenerated by implanting the rhBMP-2 retaining paste implant without bone grafting; new bone grew to restore bone loss and fix the acetabular and femoral components firmly to the host bone: and the paste implant filling the original defects was completely resorbed and replaced by newly formed bone within 12 weeks. These results were achieved with an optimized dose of rhBMP and an appropriate delivery system developed in a series of studies previously undertaken in our laboratory.[33,34]

Generally, to use rhBMP effectively for bone repair, a local delivery system is essential to elicit bone formation and define the shape of the resultant bone mass. Currently, animal-derived collagen is used as a carrier material for spinal fusion and for treating nonunions.[24–27] However, the drawbacks with collagen include lack of mechanical strength and lack of plasticity for fabrication purposes. Consequently, it is difficult to control the BMP-induced bone mass and shape, which depend on the size and shape of the carrier material. In contrast, the paste implant used in this study offers advantages over collagen in terms of mechanical characteristics that enable mass retention and plasticity. Also, the lack of potential immunoreaction and no risk for disease transmission provide safety benefits.[35–37]

To use this method clinically, the optimal dose of rhBMP required in humans must be defined. High doses of the rhBMP-2 are required to elicit new bone formation in highly evolved species including primates and humans. Milligram quantities are needed to generate a few cubic centimeters of new bone.[38] Consequently, cost becomes a barrier to broader clinical use. In our study, the dose (100 μg per defect) was much lower compared to that used in previous dog models with acetabular or femoral periprosthetic bone defects in revision THA.[39–42]

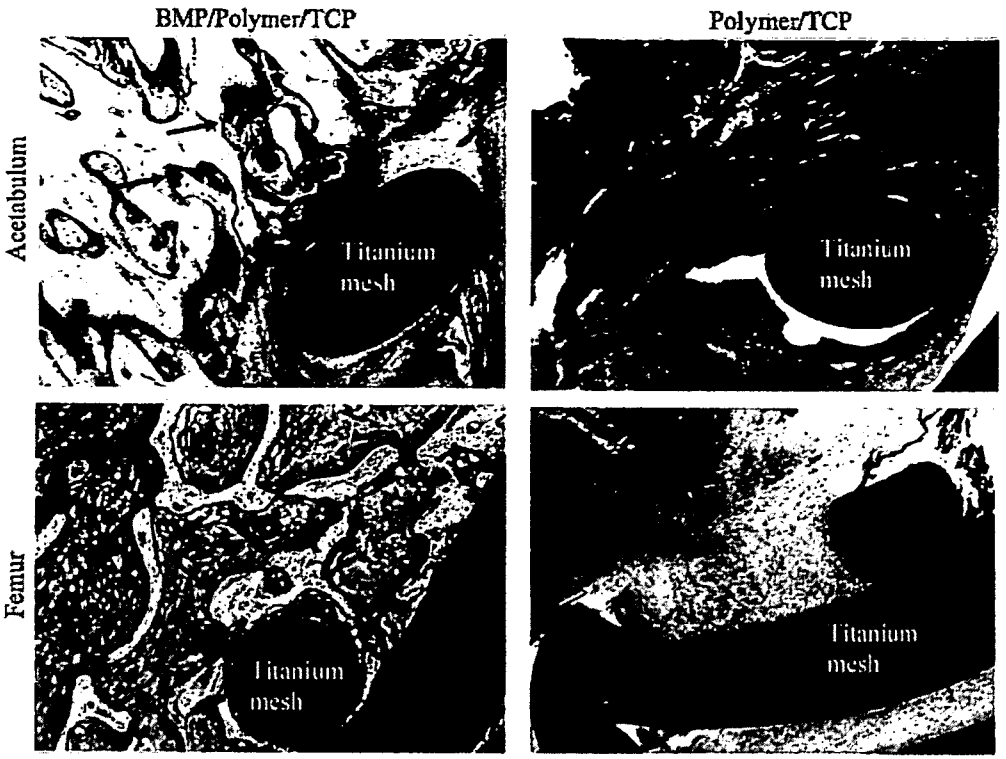

Figure 5. Undecalcified histological view at the interface between the acetabular prosthesis surface (top row) or femoral stem (lower row) and contacting tissues. In the BMP/Polymer/TCP group (left), abundant bone (arrows, stained pink) surrounds or directly contacts the prosthesis, but no bony tissue is seen in the control group (right) (Villaneuva bone stain, ×50).

Based on typical acetabular diameters in dog (2 cm) and humans (5 cm), the defects in humans are effectively 16 times larger than those in the dogs, so the required dose would be 1.6 mg. If the responsiveness to rhBMP-2 in humans is assumed to be half that in dogs, 12–13 g of the paste containing 3 to 4 mg of rhBMP-2 would be needed to repair similar types of periprosthetic defects. These

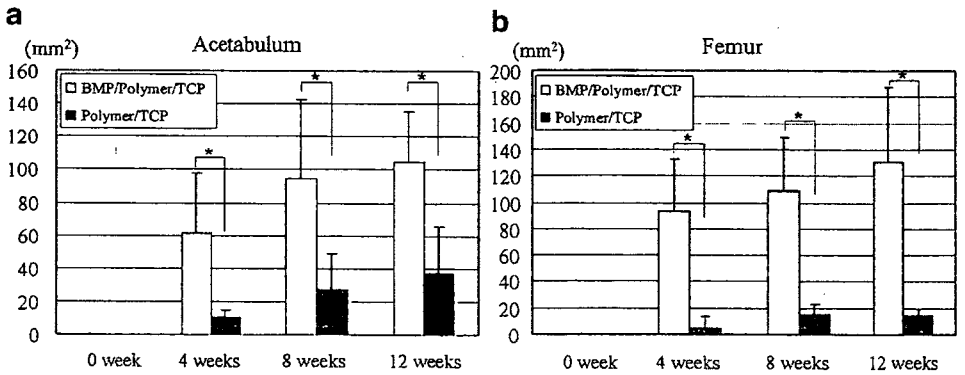

Figure 6. New bone areas (a) at the mid-coronal plane of the acetabular defects and (b) on mid-cross CT slice images of the femoral defects in the BMP/Polymer/TCP and Polymer/TCP groups at 0, 4, 8, and 12 weeks after surgery. The new bone area of the BMP/Polymer/TCP group was significantly greater than that of the Polymer/TCP group in both the acetabulum and femur at 4, 8, and 12 weeks (open columns: Significant difference, $p < 0.05$).

DOI 10.1002/jor

figures are speculative; clinical trials would be required to determine optimal dose and the safety of the rhBMP-2 used on this scale.

Addition of β-TCP to the rhBMP-2 delivery system might help repair bone defects. In a previous study, we used a sticky synthetic polymer in combination with a femoral prosthesis and rhBMP-2 to repair a proximal femoral defect.[39] In that case, mixing the rhBMP with the polymer and the combination with the prosthesis was difficult because of the highly sticky nature of the polymer. To address this limitation, biodegradable β-TCP powder was added to create putty that was easy to handle and shape. The addition of the powder reduced the effective dose of rhBMP-2 to one-fifth the amount required in the previous study to rebuild the same size femoral defect. We concluded that this delivery system was better optimized compared with the system used in our previous study.

Solid fixation of the revised prosthesis is an important factor for successful revision surgery with reduced bone stock. In our model, the acetabular socket was fixed with small screws to the anterior and posterior columns. This type of fixation may be less than required, but no displacement of the sockets was noted. This was probably due to limited or no weight-bearing pressure on the operated hip joints in the dogs for the first 2–3 week after surgery. More efforts to achieve solid fixation or limited weight bearing until a significant amount of new bone is established may be necessary as part of the clinical use of this method.

A few clinical and experimental studies have investigated the efficacy of rhBMP in revision hip surgery. Karrholm et al.[43] reported no significant clinical efficacy of rhBMP-7 (OP-1) in an impaction allograft application. In their study, OP-1 was added to morselized allograft (3.5 mg/allogeneic femoral head) as part of the impaction technique for treatment of the acetabular and femoral sides. No beneficial effects on bone formation or improved fixation were noted over 5 years. Although they did not define the reason for the lack of efficacy of OP-1, the morselized allograft might not have been an appropriate carrier material to deliver OP-1 or the dose of OP-1 may have been too low to elicit new bone formation in humans. McGee also investigated OP-1 in an impaction allograft to fix the femoral prosthesis in a sheep model.[44] Their results suggested increased allograft resorption and compromised prosthesis fixation by OP-1 addition, probably through increased remodeling activity. In another study, Barrack et al.[45] reported enhanced bone formation and partial bone ingrowth onto the porous surface of the socket by implanting an OP-1 device (rhBMP-7/Type 1 bovine collagen) in a small defect (8 mm in diameter and 5 mm in depth) in a dog model. To enhance bone ingrowth into the porous surface of an acetabular socket, Bragdon et al.[40] placed a rhBMP-2/calcium phosphate composite in the gap between the socket and the reamed acetabulum. They reported enhanced bone growth within the gap and intensified biological fixation of the socket. The results from all these studies suggest that allograft material has limited efficacy as a carrier. Alternative systems involving calcium phosphate or biodegradable polymers such as utilized in our study may be more effective.

There were some limitations in this study. The 8-month-old dogs were skeletally immature. In addition, this revision model does not include a biological response to loosening. Despite these limitations, the present study successfully achieved repair with use of a novel delivery system and an efficacious dose of rhBMP-2 determined from extensive studies conducted in our laboratory. Our findings suggest that the use of these osteoinductive, biodegradable, and absorbable implants would provide positive benefits over existing treatment procedures in revision hip surgery, specifically avoidance of bone grafts and potentially shorter recovery periods. Further studies to evaluate safety and efficacy in humans will be essential before this system can be adopted for use in the clinic.

ACKNOWLEDGMENTS

We thank Genetic Institute, Astellas Pharma Inc., Taki Chemical Co., Ltd., Olympus Biomaterial Co., Ltd., and Zimmer Japan Co., Ltd. for kindly providing the chemicals and other materials. This work was supported in part by a Grant-in-Aid from the Ministry of Education, Culture, Sports, Science and Technology of Japan (Project Grant No.30112048), Takeda Science Foundation, and the Hip Joint Foundation of Japan.

REFERENCES

1. McDonald DJ, Fitzgerald RH Jr, Ilstrup DM. 1989. Two-stage reconstruction of a total hip arthroplasty because of infection. J Bone Joint Surg Am 71-A:828–834.
2. Tsukayama DT, Estrada R, Gustilo RB. 1996. Infection after total hip arthroplasty. A study of the treatment of one hundred and six infections. J Bone Joint Surg Am 78-A:512–523.

3. Woo RY, Morrey BF. 1982. Dislocations after total hip arthroplasty. J Bone Joint Surg Am 64-A:1295–1306.
4. Dorr LD, Wolf AW, Chandler R, et al. 1983. Classification and treatment of dislocations of total hip arthroplasty. Clin Orthop Relat Res 173:151–158.
5. Warwick D, Williams MH, Bannister GC. 1995. Death and thromboembolic disease after total hip replacement. A series of 1162 cases with no routine chemical prophylaxis. J Bone Joint Surg Br 77-B:6–10.
6. Geerts WH, Heit JA, Clagett GP, et al. 2001. Prevention of venous thromboembolism. Chest 119 (Suppl):132S–175S.
7. Amstutz HC, Campbell P, Kossovsky N, et al. 1992. Mechanism and clinical significance of wear debris-induced osteolysis. Clin Orthop Relat Res 276:7–18.
8. Schmalzried TP, Guttmann D, Grecula M, et al. 1994. The relationship between the design, position, and articular wear of acetabular components inserted without cement and the development of pelvic osteolysis. J Bone Joint Surg Am 76-A:677–688.
9. Zicat B, Engh CA, Gokcen E. 1995. Patterns of osteolysis around total hip components inserted with and without cement. J Bone Joint Surg Am 77-A:432–439.
10. Whaley AL, Berry DJ, Harmsen WS. 2001. Extra-large uncemented hemispherical acetabular components for revision total hip arthroplasty. J Bone Joint Surg Am 83-A:1352–1357.
11. Berry DJ, Sutherland CJ, Trousdale RT, et al. 2000. Bilobed oblong porous coated acetabular components in revision total hip arthroplasty. Clin Orthop Relat Res 371:154–160.
12. Chen WM, Engh CA Jr, Hopper RH Jr, et al. 2000. Acetabular revision with use of a bilobed component inserted without cement in patients who have acetabular bone-stock deficiency. J Bone Joint Surg Am 82-A:197–206.
13. Head WC, Malinin TI, Emerson RH Jr, et al. 2000. Restoration of bone stock in revision surgery of the femur. Int Orthop 24:9–14.
14. Kerboull M, Hamadouche M, Kerboull L. 2000. The Kerboull acetabular reinforcement device in major acetabular reconstructions. Clin Orthop Relat Res 378:155–168.
15. Hamadouche M, Blanchat C, Meunier A, et al. 2002. Histological findings in a proximal femoral structural allograft ten years following revision total hip arthroplasty: a case report. J Bone Joint Surg Am 84-A:269–273.
16. Wolfgang GL. 1990. Femoral head autografting with total hip arthroplasty for lateral acetabular dysplasia. A 12-year experience. Clin Orthop Relat Res 255:173–185.
17. Oonishi H, Iwaki Y, Kin N, et al. 1997. Hydroxyapatite in revision of total hip replacements with massive acetabular defects: 4- to 10-year clinical results. J Bone Joint Surg Br 79-B:87–92.
18. Buck BE, Malinin TI. 1994. Human bone and tissue allografts. Preparation and safety. Clin Orthop Relat Res 303:8–17.
19. Buck BE, Resnick L, Shah SM, et al. 1990. Human immunodeficiency virus cultured from bone. Implications for transplantation. Clin Orthop Relat Res 251:249–253.
20. Wozney JM, Rosen V, Celeste AJ, et al. 1988. Novel regulators of bone formation: molecular clones and activities. Science 242:1528–1534.
21. Wang EA, Rosen V, D'Alessandro JS, et al. 1990. Recombinant human bone morphogenetic protein induces bone formation. Proc Natl Acad Sci USA 87:2220–2224.
22. Takaoka K, Yoshikawa H, Hashimoto J, et al. 1993. Purification and characterization of a bone-inducing protein from a murine osteosarcoma (Dunn type). Clin Orthop 292:329–336.
23. Takaoka K, Yoshikawa H, Hasimoto J, et al. 1993. Gene cloning and expression of a bone morphogenetic protein derived from a murine osteosarcoma. Clin Orthop 294:344–352.
24. Boden SD, Kang J, Sandhu H, et al. 2002. Use of recombinant human bone morphogenetic protein-2 to achieve posterolateral lumbar spine fusion in humans: a prospective, randomized clinical pilot trial: 2002 Volvo Award in clinical studies. Spine 27:2662–2673.
25. Burkus JK, Transfeldt EE, Kitchel SH, et al. 2002. Clinical and radiographic outcomes of anterior lumbar interbody fusion using recombinant human bone morphogenetic protein-2. Spine 27:2396–2408.
26. Friedlaender GE, Perry CR, Cole JD, et al. 2001. Osteogenic protein-1 (bone morphogenetic protein-7) in the treatment of tibial nonunions. J Bone Joint Surg Am 83-A (Suppl 1):S151–S158.
27. Govender S, Csimma C, Genant HK, et al. 2002. Recombinant human bone morphogenetic protein-2 for treatment of open tibial fractures: a prospective, controlled, randomized study of four hundred and fifty patients. J Bone Joint Surg Am 84-A:2123–2134.
28. Miyamoto S, Takaoka K, Okada T, et al. 1993. Polylactic acid-polyethylene glycol block copolymer. A new biodegradable synthetic carrier for bone morphogenetic protein. Clin Orthop 294:333–343.
29. Saito N, Okada T, Toba S, et al. 1999. New synthetic absorbable polymers as BMP carriers: plastic properties of poly-D,L-lactic acid-polyethylene glycol block copolymers. J Biomed Mater Res 47:104–110.
30. Saito N, Okada T, Horiuchi H, et al. 2001. Biodegradable poly-D,L-lactic acid-polyethylene glycol block copolymers as a BMP delivery system for inducing bone. J Bone Joint Surg Am 83-A (Suppl 1):S92–S98.
31. D'Antonio JA, Capello WN, Borden LS, et al. 1989. Classification and management of acetabular abnormalities in total hip arthroplasty. Clin Orthop Relat Res 243:126–137.
32. D'Antonio J, McCarthy JC, Bargar WL, et al. 1993. Classification of femoral abnormalities in total hip arthroplasty. Clin Orthop Relat Res 296:133–139.
33. Namikawa T, Terai H, Suzuki E, et al. 2005. Experimental spinal fusion with recombinant human bone morphogenetic protein-2 delivered by a synthetic polymer and beta-tricalcium phosphate in a rabbit model. Spine 30:1717–1722.
34. Kato M, Namikawa T, Terai H, et al. 2006. Ectopic bone formation in mice associated with a lactic acid/dioxanone/ethylene glycol copolymer-tricalcium phosphate composite with added recombinant human bone morphogenetic protein-2. Biomaterials 27:3927–3933.
35. Bach FH, Fishman JA, Daniels N, et al. 1998. Uncertainty in xenotransplantation: individual benefit versus collective risk. Nat Med 4:141–144.
36. Butler D. 1998. Last chance to stop and think on risks of xenotransplants. Nature 391:320–324.
37. DeLustro F, Dasch J, Keefe J, et al. 1990. Immune responses to allogeneic and xenogeneic implants of

DOI 10.1002/jor

collagen and collagen derivatives. Clin Orthop Relat Res 260:263–279.
38. Valentin-Opran A, Wozney J, Csimma C, et al. 2002. Clinical evaluation of recombinant human bone morphogenetic protein-2. Clin Orthop Relat Res 395:110–120.
39. Murakami N, Saito N, Takahashi J, et al. 2003. Repair of a proximal femoral bone defect in dogs using a porous surfaced prosthesis in combination with recombinant BMP-2 and a synthetic polymer carrier. Biomaterials 24:2153–2159.
40. Bragdon CR, Doherty AM, Rubash HE, et al. 2003. The efficacy of BMP-2 to induce bone ingrowth in a total hip replacement model. Clin Orthop Relat Res 417:50–61.
41. Sumner DR, Turner TM, Urban RM, et al. 2004. Locally delivered rhBMP-2 enhances bone ingrowth and gap healing in a canine model. J Orthop Res 22:58–65.
42. Sumner DR, Turner TM, Urban RM, et al. 2006. Additive enhancement of implant fixation following combined treatment with rhTGF-beta2 and rhBMP-2 in a canine model. J. Bone Joint Surg Am 88-A:806–817.
43. Karrholm J, Hourigan P, Timperley J, et al. 2006. Mixing bone graft with OP-1 does not improve cup or stem fixation in revision surgery of the hip: 5-year follow-up of 10 acetabular and 11 femoral study cases and 40 control cases. Acta Orthop 77:39–48.
44. McGee MA, Findlay DM, Howie DW, et al. 2004. The use of OP-1 in femoral impaction grafting in a sheep model. J Orthop Res 22:1008–1015.
45. Barrack RL, Cook SD, Patron LP, et al. 2003. Induction of bone ingrowth from acetabular defects to a porous surface with OP-1. Clin Orthop Relat Res 417:41–49.